Agricultural and Forest Meteorology 349 (2024) 109960

Contents lists available at ScienceDirect

Agricultural and Forest Meteorology

journal homepage: www.elsevier.com/locate/agrformet

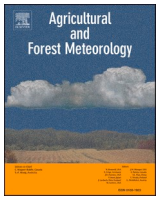

Energy availability and leaf area dominate control of ecosystem evapotranspiration in the southeastern U.S.

Maricar Aguilos [a,*], Ge Sun [b], Ning Liu [c], Yulong Zhang [b], Gregory Starr [d], Andrew Christopher Oishi [e], Thomas L O'Halloran [f,j], Jeremy Forsythe [f,j], Jingfeng Wang [g], Modi Zhu [g], Devendra Amatya [h], Benju Baniya [i], Steve McNulty [b], Asko Noormets [i], John King [a]

[a] Department of Forestry and Environmental Resources, North Carolina State University, Raleigh, NC 27695, USA
[b] Eastern Forest Environmental Threat Assessment Center, Southern Research Station, USDA Forest Service, Research Triangle Park, NC 27709, USA
[c] CSIRO Environment, Canberra, ACT, Australia 2601
[d] Department of Biological Sciences, University of Alabama, Tuscaloosa, AL 35487, USA
[e] Coweeta Hydrologic Laboratory, Southern Research Station, USDA Forest Service, Otto, NC 28763 USA
[f] Baruch Institute of Coastal Ecology & Forest Science, Clemson University, Clemson, SC 29440, USA
[g] School of Civil and Environmental Engineering, Georgia Institute of Technology, Atlanta, GA 30332, USA
[h] Center for Forest Watershed Research, Southern Research Station, USDA Forest Service, Cordesville, SC 29434, USA
[i] of Ecosystem Science and Management, Texas A&M University, College Station, TX 77843-2138, USA
[j] Department of Forestry & Environmental Conservation, Clemson University, Clemson, SC 29634-0317, USA

ARTICLE INFO

Keywords:
Eddy covariance
Modeling
Land-use change
Budyko
Machine learning

ABSTRACT

Evapotranspiration (ET) links water, energy, and carbon balances, and its magnitude and patterns are changing due to climate and land use change in the southeastern U.S. Quantifying the environmental controls on ET is essential for developing reliable ecohydrological models for water resources management. Here, we synthesized eddy covariance data from 24 AmeriFlux sites distributed across the southeastern U.S., comprising 162 site-years of flux data representing six representative ecosystems including cropland vegetation mosaic (CVM), deciduous broadleaf forests (DBF), evergreen needle-leaf forests (ENF), grasslands (GRA), savannas (SAV), and wetlands (WET). Our objectives were to assess the daily, seasonal, and annual variability in ET and to develop practical predictive models for regional applications in ecosystem service analysis. We evaluated the response of ET to climatic and biotic forcings including potential evapotranspiration (PET), precipitation (P), and leaf area index (LAI), and compared the performance of these empirical ET models based and those developed using machine learning algorithms. Our results showed that the mean daily ET varied significantly, ranging from 1.36 mm d^{-1} in GRA to 2.30 mm d^{-1} in SAV, with a numerical order : GRA < DBF < ENF < WET < CVM < SAV. In this humid region, mean annual PET exceeded P in 16 out of the 24 flux sites. Using the Budyko framework, we showed that ENF had the highest evaporative efficiency (ET/P). PET and leaf area index (LAI) emerged as the most influential factors explaining ET variability. Artificial neural networks (ANN) and random forest (RF) models demonstrated superior capabilities in predicting monthly ET across sites over generalized additive modeling (GAM) and multiple linear regression (MLR) methods. The present study confirmed that the Southeast region is generally 'energy limited', implying that atmospheric demand along with vegetation information can be used to reliably estimate monthly and annual ET. Our study provides valuable insights into how ET of specific ecosystems is controlled by climatic and land surface drivers, enabling the development of reliable predictive models for regional extrapolation of flux measurements in water resource management in the humid southeastern U.S. region.

* Corresponding author at: 2820 Faucette Drive, 1025 Biltmore Hall, Raleigh, NC 27695, USA.
E-mail address: mmaguilo@ncsu.edu (M. Aguilos).

https://doi.org/10.1016/j.agrformet.2024.109960
Received 14 August 2023; Received in revised form 29 February 2024; Accepted 3 March 2024
Available online 7 March 2024

1. Introduction

Evapotranspiration (ET) serves as a crucial link among hydrological, biological, and ecological processes (Abdullah et al., 2015; Bhattarai and Wagle, 2021; Feng et al., 2017; Sun et al., 2016) and is an important indicator of ecosystem functioning and for quantifying ecosystem services (Sun et al., 2017). Consequently, understanding ET becomes vital for comprehending ecosystem responses to global environmental change (Acharya et al., 2022; Fisher et al., 2017; Mu et al., 2011). However, accurately estimating ET dynamics including its components (i.e., canopy interception, soil and understory evaporation, and transpiration) remain highly uncertain, especially for vegetated surfaces where ET is governed by multiple biophysical processes operating at multiple scales (Anapalli et al., 2018; Chai et al., 2018; Fang et al., 2016; Negm et al., 2018; Sun et al., 2011a; Zhang et al., 2018).

Despite being a humid and water-rich region, the southeastern U.S. is not immune to water shortages resulting from climate change and increasing water demand (Engström et al., 2021; Sun et al., 2008). Forest-dominated headwater streams, which supply water, have declined due to elevated atmospheric demand, a longer growing season, and shifts in tree species composition (Caldwell et al., 2016; McQuillan et al., 2022), and groundwater losses (Engström et al., 2021). On the other hand, to mitigate the hydrological impacts of climate change and enhance ecosystem resilience in energy-limited environment like the higher elevation forest ecosystems, management strategies such as prescribed burning, thinning, and forest ecosystem restoration should incorporate vegetation management practices that specifically target the reduction of water usage as ET (Ma et al., 2020; Mclaughlin et al., 2013).

However, there is a large spatial and temporal variability of water fluxes across the U.S. Southeast due to high spatial and temporal variability in climate, vegetation dynamics, and land management regimes (Aguilos et al., 2021a; Stoy et al., 2006; Sun et al., 2010). Moreover, the complex terrains and diverse ecosystem structures in ecoregions such as the Appalachian Mountains, Piedmont, and Coastal Plains make accurate ET estimation challenging (Aguilos et al., 2022; Amatya et al., 2016b; Oishi et al., 2018; Sun et al., 2011b). ET measurements across regional gradients and different environmental conditions (e.g. climate, soil types, elevation, hydrologic setting) spanning various ecosystem biomes (e.g. grasslands, savannas, agricultural lands, forests), and in some cases management practices (harvesting, thinning, prescribed fire), are required to develop reliable regional ecohydrological models for water resources management, particularly for the loss of water through ET to mitigate vegetation stress responses under climatic change (Acharya et al., 2022; Fang et al., 2016; Fisher et al., 2017).

ET is influenced by various climatic factors, such as air temperature, net radiation, vapor pressure deficit (VPD), wind speed, rainfall, and other biotic variables, along with stomatal behavior (Adnan et al., 2020; Aguilos et al., 2021a, 2018b; Fang et al., 2016). Daily ET is also affected by soil water storage, which is dependent upon interactions between seasonal ET rates and precipitation (Aguilos et al., 2021b; Noormets et al., 2010, 2008). Any changes in soil hydro-physical properties also affect ET (Nobrega et al., 2017). Among the biotic drivers of ET, leaf area index (LAI) is a primary control of forest structure (Acharya et al., 2022) and vegetation growth, and an increase in LAI can potentially lead to both higher potential evapotranspiration (PET) as well as ET rates (Malone et al., 2015). Species composition, canopy structure (open or closed), age (young or old), and edge effects may also affect ET rates, as they influence light availability and to some degree, turbulence reaching the forest floor (Ringgaard et al., 2012). PET, a climatic parameter, is an essential input for hydrologic models and serves as a significant variable in determining actual ET (Amatya et al., 2016a; Xu and Singh, 2004). Elevation is an underexplored factor affecting ET rates, yet its significant role in regional meteorology has been acknowledged (Sun et al., 2020). However, the specific response of ET to the changing climate, with variation in elevation remains unclear.

Directly quantifying ET fluxes using the eddy covariance method in the southern U.S. began in the early 1990s (Gholz and Clark, 2002). Eddy covariance (EC) techniques enable the direct measurement of ET fluxes at the stand scale (Paul-Limoges et al., 2015; Soubie et al., 2016). However, EC systems are expensive (Markwitz and Siebicke, 2019), which limits the use of this technique to estimate ET. Remote sensing has been employed to estimate global ET (Bhattarai and Wagle, 2021; Chen and Liu, 2020; Yang et al., 2017), however, this method encounters various challenges, including limited applicability and consistency under diverse conditions (Bhattarai and Wagle, 2021; Hu et al., 2020) and a scarcity of calibration and validation datasets (Fisher et al., 2017). Mathematical modeling has been widely used to enhance our understanding of ET and scaling up (Fang et al., 2016; Granata, 2019; Komatsu and Kume, 2020; Sun et al., 2011b; Yaseen et al., 2019). Machine learning algorithms, such as Artificial Neural Networks (ANN) (Nema et al., 2017; Stangierski et al., 2019), Generalized Additive Modeling (GAM) (Markos and Radoglou, 2023), and Random Forest (RF) (Chen et al., 2020), have already been used in evapotranspiration research (Mehdizadeh, 2018; Nema et al., 2017; Xu et al., 2018). However, the current applications of machine learning techniques for estimating ET are limited, and our understanding of the topic is still partial and fragmented (Granata, 2019). ET models have been used to capture the fundamental biophysical controls of ET, such as from LAI, water, and energy availability (Fang et al., 2016; Feng et al., 2012; Komatsu and Kume, 2020). However, these models also face challenges due to their inherent limitations and deficiencies. For example, some studies overlooked the biome-specific physiological characteristics of ET processes by employing a single global ET model equation for all land cover types (Mackay et al., 2007; Sun et al., 2011a). In contrast, other studies aimed to address this issue by developing land cover-specific ET models within a global context (Fang et al., 2016). These models did not fully account for the fact that biomes, although often regarded as distinct regions, lack clearly delineated boundaries.

Modeling ET in hydrology at a large spatial scale remains challenging due to the difficulty in characterizing the landscape heterogeneity, diverse plant traits that control stomatal regulation, and ecohydrological data availability for model calibration and validation. One study highlighted a need to quickly detect emerging environmental challenges and then develop practical models for connecting different stakeholders (Komatsu and Kume, 2020). To address this issue, we conducted a regional synthesis of ET by collating data from eddy flux tower sites across the southeastern U.S. over six ecosystems (i.e., savannas, grasslands, croplands, conifer and broadleaf forests, and wetlands). Our main goal is to determine the major controls over ET and use them to develop a practical land cover-specific ET model within a regional context, especially in this humid and water-rich region – the southeastern U.S.

Our specific objectives were to (1) determine the daily, seasonal, and annual variability of ET across different ecosystems; (2) evaluate the functional response of ET to climatic and biological forcings; (3) characterize site-level variation in evaporative and dryness indices using the Budyko framework (Budyko, 1974); and (4) compare the performance of both empirical and machine learning based ET predictive models. We hypothesized that (1) spatial and temporal variability in ET will be affected by elevation, LAI, P, and PET; (2) PET may have more control over ET than precipitation in this non-water-limited region; and (3) models developed specifically for each land cover type will have better model performance compared to lumped ecosystems model. Our synthesis study highlights the importance of using land cover-specific ET models for regional applications and provides insights into how ET of specific ecosystems responds to climatic drivers in a time of rapid change.

2. Methods

2.1. Eddy flux data

Eddy covariance data were obtained from the AmeriFlux network.

The Level 4 data product for 24 sites, encompassing 162 site-years of data, were downloaded (Supplemental Table 1, Fig. 1). These sites cover a diverse array of vegetation types, including evergreen needleleaf forests (ENF), deciduous broadleaf forests (DBF), savannas (SAV), wetlands (WET), croplands (CVM), and grasslands (GRA) (Table 1).

Erroneous data are common issues in flux measurements (Aguilos et al., 2018a, 2014; Soloway et al., 2017). To address this issue, we took the following data filtering steps (Fig. 2): 1) We removed the data when daily net radiation (Rn) exceeded 100 MJ m^{-2}, as well as when daily LE or H exceeded 25 MJ m^{-2}. 2) We also excluded the data when the calculated daily PET was negative, ET exceeded 300 mm month^{-1}, or Rn was negative.

2.2. Input variables

Daily ET taken from the eddy flux system represents the canopy evaporation, transpiration, and soil evaporation. ET was converted from latent heat flux (LE in W m^{-2}) (Aguilos et al., 2021a; Sun et al., 2011b) using the conversion factor of LE (W m^{-2}) to ET (mm day^{-1}) considering the 30-minute time interval:

$$ET = \frac{LE}{\lambda} \quad (1)$$

where, λ (J kg^{-1}) = 10^3 * (2500 – 2.37 * Ta), Ta = Air temperature in °C (Celsius).

Daily ET was the sum of 30-min ET and compiled as the monthly average or sum, depending on the context and timescale we needed for the analysis. A year with more than one month gap was discarded from the analysis. Gaps of a few days were gapfilled using linear interpolation.

Potential evapotranspiration (PET) was estimated using the Priestley-Taylor method (Ponraj and Vigneswaran, 2020) as it is simpler and input variables are more readily available compared to the Penman-Montieth method (Montieth, 1965). The Priestley-Taylor equation ((Priestley and Taylor, 1972) is given by:

$$PET = \alpha \frac{\Delta\ (R_n - G)}{\lambda_v\ (\Delta + \gamma)} \quad (2)$$

Table 1
Ecosystem descriptions as defined from Ameriflux network (https://ameriflux.lbl.gov/).

Ecosystem	Site Description
CVM	Cropland/Natural Vegetation Mosaics: Lands with a mosaic of croplands, forest, shrublands, and grasslands in which no one component comprises more than 60% of the landscape
DBF	Deciduous Broadleaf Forests: Lands dominated by woody vegetation with a percent cover >60% and height exceeding two meters. Consists of broadleaf tree communities with annual cycle of leaf-on and leaf-off periods
ENF	Evergreen Needleleaf Forests: Lands dominated by woody vegetation with a percent cover >60% and height exceeding two meters. Almost all trees remain green all year. Canopy is never without green foliage
GRA	Grasslands: Lands with herbaceous types of cover. Tree and shrub cover is less than 10%. Permanent wetlands lands with a permanent mixture of water and herbaceous or woody vegetation. The vegetation can be present in either salt, brackish, or fresh water.
SAV	Savannas: Lands with herbaceous and other understory systems, and with forest canopy cover between 10 and 30%. The forest cover height exceeds two meters
WET	Permanent Wetlands: Lands with a permanent mixture of water and herbaceous or woody vegetation present in either salt, brackish, or fresh water

In this equation, PET is the potential evapotranspiration in mm d^{-1}, α is an empirical constant accounting for the vapor pressure deficit and resistance values. We used a constant of 1.26 from the original method, typically used for open bodies of water, but with a wide range of values from less than 1 (humid conditions) to almost 2 (arid conditions). λ_v is the volumetric latent heat of vaporization, 2453 MJ m^{-3}. Δ is the slope of the saturation vapor pressure-temperature curve (kPa per°C). γ is the psychometric constant (kPa per°C). Ameriflux database provides *Rn* and soil heat flux (*G*) in W m^{-2}. However, Eq. (2) requires *Rn* and *G* in MJ m^{-2} d^{-1}. Thus, we convert W m^{-2} into MJ m^{-2} d^{-1} using the conversion factor: 1 W m^{-2} = 0.0864 MJ m d^{-1}.

LAI was bi-linearly interpolated to estimate daily LAI values from fused Moderate Resolution Imaging Spectroradiometer (MODIS) 500 m and Landsat 30 m LAI (Yang et al., 2017). Daily precipitation (P), air temperature (Tair), net radiation (Rn), and vapor pressure deficit (VPD)

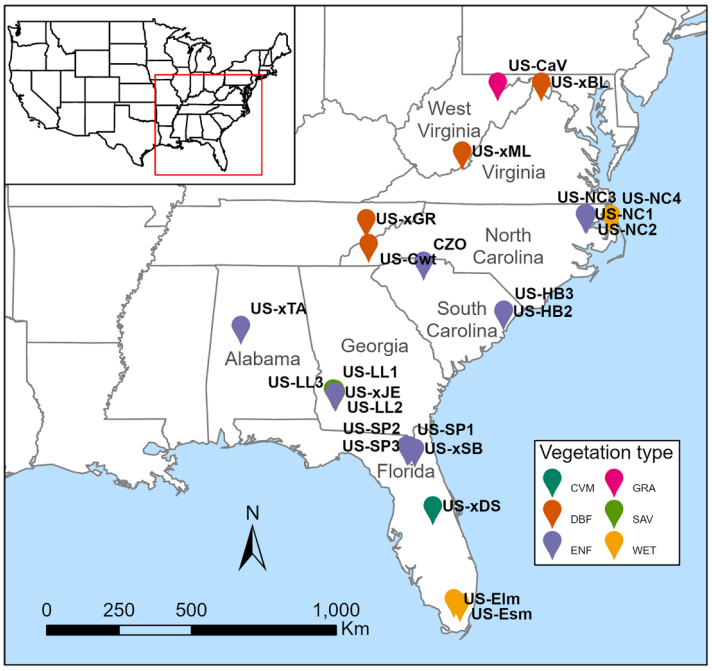

Fig. 1. Location of carbon flux towers across the Southeast U.S. Ecosystems include CVM (Crop Vegetation Mosaic); DBF (Deciduous Broadleaf Forests); ENF (Evergreen Needleleaf Forests); GRA (Grasslands); SAV (Savannas); and WET (Wetlands).

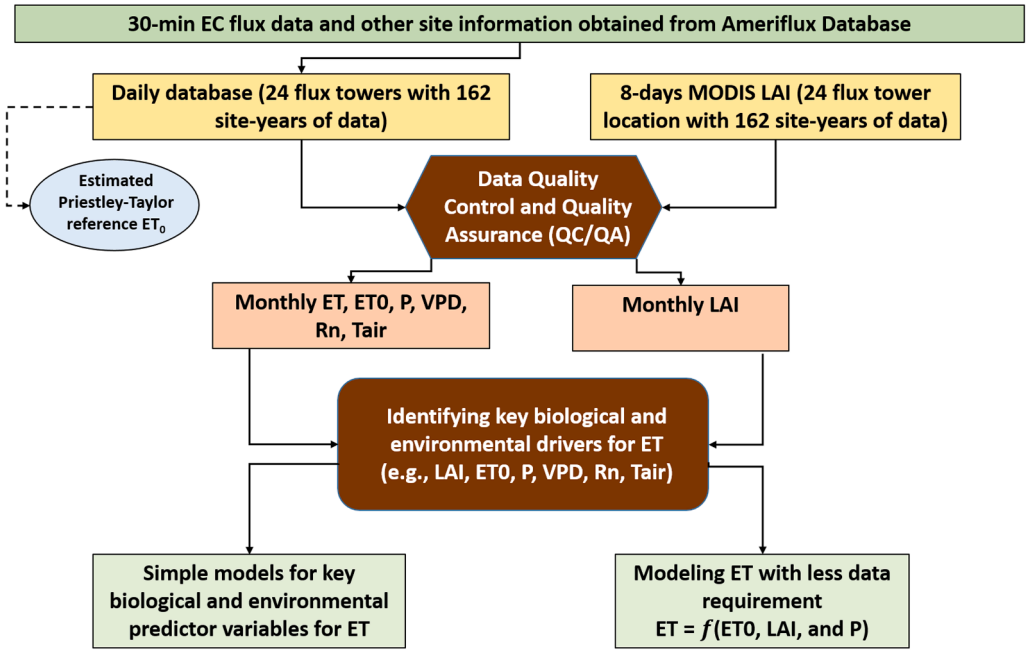

Fig. 2. The process flow of database content development, processing, and analysis.

were obtained from the flux tower data.

2.3. Modeling monthly ET

Following the approaches of (Fang et al., 2016) and (Sun et al., 2011a), we used three variables, namely potential evapotranspiration (PET), leaf area index (LAI), and precipitation (P), to build predictive ET models. The selected models included the Multiple Regression (MR), Artificial Neural Network (ANN), Generalized Additive Modeling (GAM), and Random Forest (RF) models. These models were chosen due to their demonstrated high performance and capacity to "learn" complex, highly non-linear relationships. We included the variables of *Rn, VPD*, and *Tair* to investigate the functional response of evapotranspiration to climatic and biological forcings.

2.3.1. Multiple regression method

Multiple linear regression is a widely-used regression model known for simplicity and effectiveness (Xuanxuan, 2018). It can be represented by Eq. (3), where β_0 denotes the intercept, β_1, β_2, …, β_n represent the regression model coefficients, and ε accounts for the multivariate error (Uyanık and Güler, 2013).

$$Y = \beta_0 + \beta_1 X_1 + \beta_2 X_2 \ldots\ldots + \beta_n X_n + \varepsilon \quad (3)$$

2.3.2. Generalized additive model (GAM)

Generalized Additive Modeling (GAM) is a flexible and smoothing technique that captures data non-linearities in data fitting. The influence of each covariate is captured through a smoothing function (Aguilos et al., 2018a; Markos and Radoglou, 2023; Shao et al., 2015). In this analysis, we used the spline function for smoothing covariates. The second-order Akaike information criterion (AIC) was used to avoid model over-parameterization (Burnham et al., 2011) and to slightly adjust the first-order bias-corrected AIC to reduce the bias (Burnham et al., 2011; Yanagihara et al., 2023). The *gam* function from the *mgcv* package in R was adopted to build the statistical models, and the *MuMin* package assisted in obtaining the best smoothing dimension (Barton, 2022).

The following formula represents the GAM model:

$$ET = f_1(ET_o) + f_2(LAI) + f_3(P) + \varepsilon \quad (4)$$

where f_1, f_2, and f_3 are the smooth functions estimated by the model for each of the predictor variables, and ε is the error term.

2.3.3. Random forest (RF)

Random Forest (RF) uses decision trees to create a forest (Chen et al., 2020; Ponraj and Vigneswaran, 2020). Decision trees represent all possible outcomes of a decision using a branching approach. RF relies on two crucial parameters: the node of a tree that defines the full features used, and the number of trees in the forest. By introducing randomness, this model effectively avoids overfitting issues (Hu et al., 2020).

Similar to the MLR method, we used PET, LAI, and P to train a random forest regressor on ET within the training set. The performance of RF was then tested using the validation set. During the construction of random forests, the bootstrap method was applied to randomize the use of variables (columns) and the use of data (rows). The new sample is classified using the trained set of classifiers. Then the classification results for all classifiers are counted by the mean of the output, and the highest categories are the final tag (Chen et al., 2020). With these three sets of parameters needed in RF regression, we set the minimum sample leaf to 100, the number of decision trees to 500, and the feature attributes to three. We used the *randomForest* package in R to train and verify the model (Liaw and Wiener, 2002). These parameters were applied to the entire dataset and for each ecosystem type.

2.3.4. Artificial neural network (ANN)

The Artificial Neural Network (ANN) employs a multi-layer perceptron network with backpropagation that consists of an input layer, one hidden layer, and one output layer. The number of input layer nodes corresponds to the variables describing the attributes being tested, while the number of neurons in the output layer is equal to the number of classes (Fig. 3). The complexity of the task and the available training data determine the number of hidden layers and neurons in the model (Nema et al., 2017; Stangierski et al., 2019).

This study used a total of 1944 monthly data records, where 60% were used as training datasets and the remaining 40% as validation set in a three-layer feed-forward back propagation algorithm. The supervised learning of the model was done using ET as output and PET, LAI, and P as input parameters. We optimized the model for each ecosystem type using the *neuralnet* package in R (Fritsch et al., 2019).

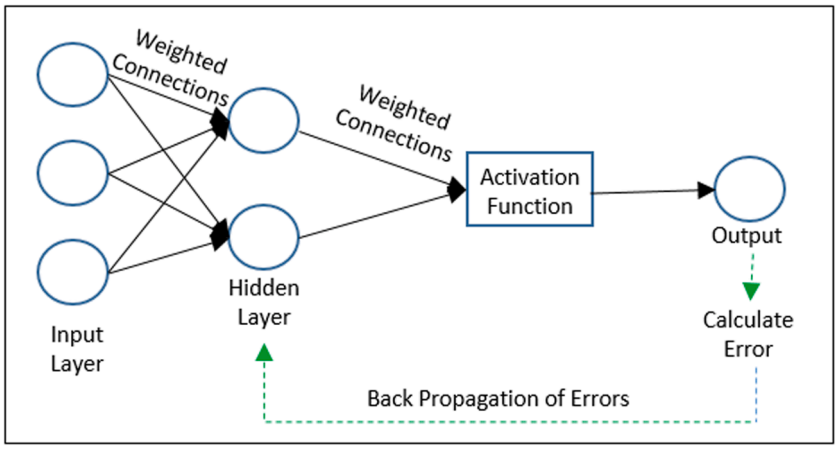

Fig. 3. A diagram for building a neural network model.

2.4. Model accuracy assessment

To compare the performance of different models, we used two widely used indicators: the coefficient of determination (R^2) and the root mean square error (RMSE). These metrics serve to evaluate the agreement between the estimated and observed values of ET. The R^2 quantifies the proportion of the variance in ET that can be explained by PET, LAI, and P. A value of R^2 closer to 1.0 means the higher correlation between observed and modeled ET. On the other hand, RMSE is a measure of the average distance between the predicted and observed ET. The lower the RMSE, the better a given model can fit the dataset. We also compared model performances using the Akaike Information Criterion (AIC). The AIC compares the quality of a set of statistical models to each other. The AIC will rank each model from best to worst, thus providing the means for model selection.

2.5. Addressing collinearity issues

In the regression models, collinearity issues arise among the independent input variables, which should be addressed. We computed the variance inflation factor (VIF) (Fang et al., 2016) to identify highly correlated variables. Any variable with a high VIF value (above 5 or 10) should be removed from the model, leading to a simpler model without compromising the model's accuracy. Theoretically, PET, Rn, VPD, and T_{air} are all energy-related climatic variables that are confounded and tightly coupled. For example, PET and Rn, and possibly T_{air} were highly correlated. Their VIF values with ET showed a VIF = > 5, indicating collinearity issues. We chose PET,that integrates temperature and net radiation together, among these energy-related variables to reduce the multicollinearity issue. We then added the LAI (a biological parameter) and P (that influences both canopy evaporation as well as soil moisture-related variable) as input to simplify model development for ET. Besides, PET, LAI, and P have been used by many authors and can be readily obtained from standard weather stations or as remote sensing data products(Sun et al., 2011b; Xu and Singh, 2005).

2.6. The budyko framework

We put our mean annual ET data in the context of the Budyko framework (Chen and Sivapalan, 2020; Kirschbaum, 2017; Sposito, 2017) to demonstrate the influence of the aridity index (PET/P) on the water use strategies and efficiency (ET/P) of various ecosystems. Several mathematical forms are available to describe the relationship between evaporative and dryness indices. For example, (Zhang et al., 2001) used an equation to show that long-term mean forests ET is higher than grass ET (see Eq. (5)). In this model, *ET* is evapotranspiration, *PET* is the potential evapotranspiration, *P* is precipitation, and the plant available water coefficient is denoted by *w*. The parameter *w* was determined as 2.0 for all types of forests and 0.5 for grasslands, including savannah (Zhang et al., 2001).

$$\frac{ET}{P} = \frac{1 + w\frac{PET}{P}}{1 + w\frac{PET}{P} + \frac{P}{PET}} \tag{5}$$

Another form of Budyko curve was developed by (Fu, 1981) where the *w* parameter value of 2.84 was found to best fit data for forests and 2.55 for grass-dominated watersheds (Zhang et al., 2004).

$$\frac{ET}{P} = 1 + \frac{PET}{P} - \left[1 + \left(\frac{PET}{P}\right)^{w}\right]^{1/w} \tag{6}$$

We used these two Budyko models above to determine our optimized *w* using our datasets for various ecosystems to examine how our sites in the southeastern U.S. differ from the mean ET of other global ecosystems represented by the Budyko models. We then determine the coefficient of determination for the Budyko models and our optimized model to make comparisons.

3. Results

3.1. Variability in biological and climate variables across elevational gradients

Higher-elevation ecosystems include DBF (~200 m asl to >1000 m asl) and GRA (~900 m asl), while the remaining ecosystems were at lower elevations (~0.4 m asl to ~180 m asl; Fig. 4a). The 1000 mm mean annual P isoline separated the GRA and SAV ($P < 1000$ mm) from the CVM, DBF, and WET ($P > 1000$ mm). The 15.0 °C mean annual temperature threshold separated the GRA and DBF (< 15.0 °C) from ENF, CVM, and SAV (>15.0 °C) and mainly occurred at mid- to high-elevation ranges (Fig. 4b).

Across all ecosystem types, GRA had the lowest monthly PET (56.5 mm month $^{-1}$) while SAV had the highest (117.6 mm month $^{-1}$) (Fig. 5, Supplemental Table 2). GRA also had the lowest precipitation (75.0 mm month^{-1}), while the CVM and DBF sites received higher monthly P of 107.9 mm month^{-1} and 104.7 mm month^{-1}, respectively. ENF sites had the highest average LAI (4.1). GRA ecosystems had the lowest average net radiation with only 59.2 W m$^{-2,}$ while the rest had an average Rn ranging from 112.14 W m^{-2} to 130.03 W m^{-2}. The average VPD among all ecosystem types was 0.65 kPa while air temperature varied from 8.0°C to 22.8°C.

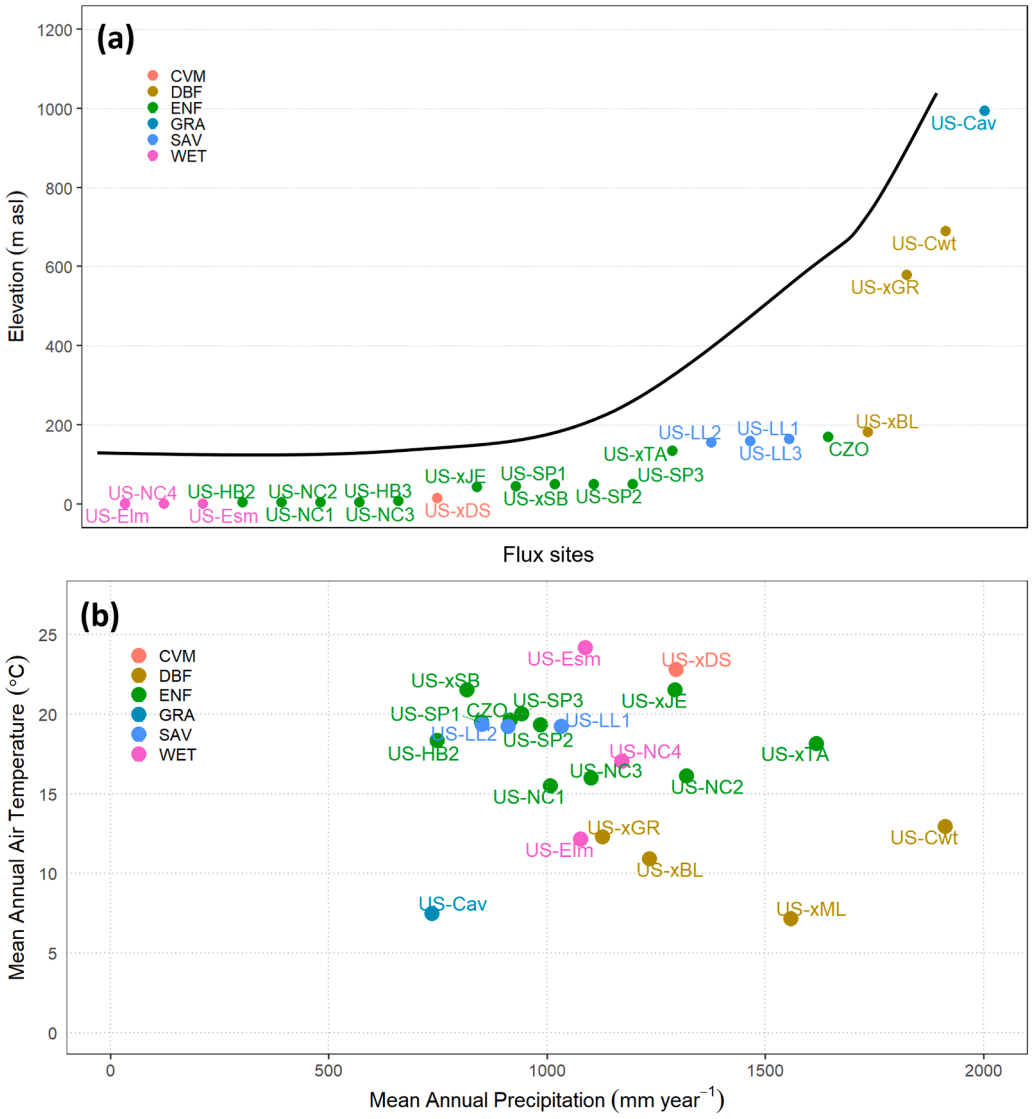

Fig. 4. The different ecosystems across elevational gradients (a) and the distribution of mean annual temperature and annual mean precipitation across various ecosystem (b). Ecosystems include CVM (Crop Vegetation Mosaic), DBF (Deciduous Broadleaf Forest), ENF (Evergreen Needleleaf Forest), GRA (Grassland), SAV (Savannas), and WET (Wetland).

3.2. Daily, seasonal, and annual variations in et

Our results showed that mean daily ET varied significantly from 1.36 mm d^{-1} in GRA to 2.30 mm d^{-1} in CVM (Fig. 6), with a trend of GRA < DBF < ENF < WET < CVM < SAV ($p < 0.05$). There were significant differences in ET among grass, deciduous forests, and evergreen forests. It is interesting to note that the highest daily ET was found in Savanna indicating climatic effects on ET.

The seasonal variations in ET followed a trend of increasing ET from January to May, peaking during the summer, and gradually declining towards September to December (Fig. 7a). Lower elevation (< 200 m asl) ecosystems (e.g., WET, CVM, SAV, and ENF) released low amounts of water during the non-growing seasons of only 1.0 mm d^{-1} to 2.0 mm d^{-1}, and even lesser amount at the higher elevation (> 200 m asl) ecosystems, such as DBF and GRA, at < 1.0 mm d^{-1}. Higher rainfall during the winter (November to December) at mid-elevation sites did not result in higher ET rates (Figs. 7a and 7b). The ET fluxes were the highest during the peak of the growing season (June to August) and consumed 58 – 82% of P when temperature was high (Fig. 7c).

The highest P was recorded in CVM sites (mean annual = 1295 mm), which was similar to the DBF sites (1256 mm), while the lowest P of 900 mm was mainly in Virginia's Canaan Valley GRA sites. The P distribution varied mostly in DBF sites (674 mm – 1870 mm), located along an elevation gradient from 183 m asl to 1126 m asl. The CVM sites also had the highest mean annual ET (819 mm), with the lowest (489 mm) for the GRA site. However, the site with the widest range of annual mean ET was ENF, ranging from 436 mm to 1327 mm (mean = 796 mm). CVM also had the highest mean annual PET (1451 mm), but the highest PET variability occurred in DBF sites, with a 910 mm difference between the minimum of 652 mm and a maximum of 1562 mm. While mean annual PET tended to be higher than the mean annual P in most ecosystems, this was not the case for higher elevation sites such as DBF and GRA, where higher rainfall amounts were recorded than the PET (Table 2). Out of 24 flux sites, 16 sites had P that exceeded PET. The pine plantations (US-NC2 and US-NC3), a natural forest (US-xTA), a wetland in North Carolina (US-NC4), Virginia's deciduous broadleaf forests (US-xML and US-xBL), and grassland site (US-CaV) all had PET lower than P.

On an annual basis across all sites, mean annual P explained 12% of the variations in ET while PET explained 32% (Fig. 8, equation not shown). Mean annual ET was generally lower than calculated PET (Fig. 8). Indicative of the warm and wet climate conditions, the Southeast U.S. had an overall annual ET:P of 0.44 to 0.89, but high PET:P

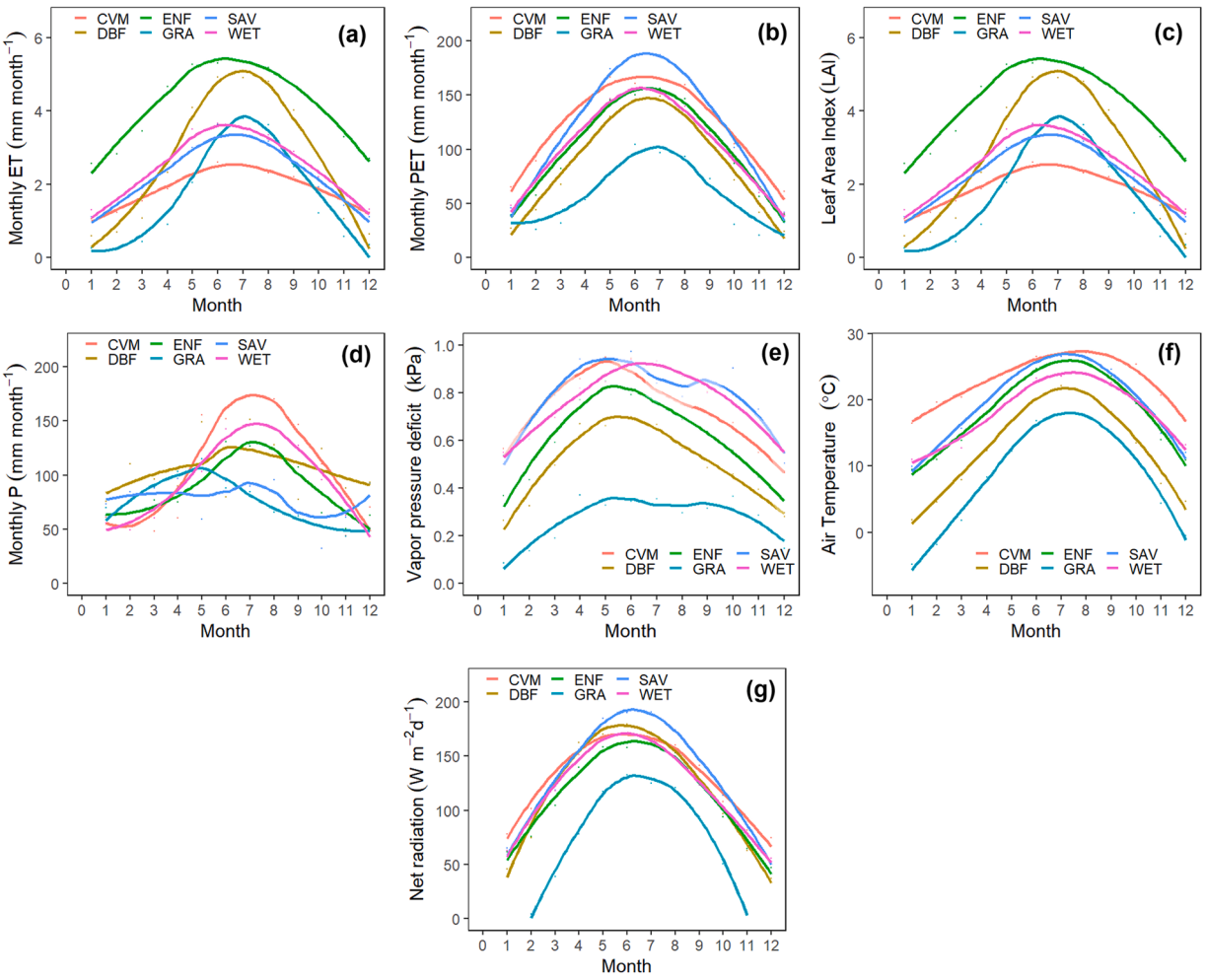

Fig. 5. Variation in biological and climatic input variables), (a) PET (potential evapotranspiration), (b) Monthly P, (c) LAI (leaf area index), (d) Tair (air temperature), (e) Rn (net radiation), and (f) VPD (vapor pressure deficit).

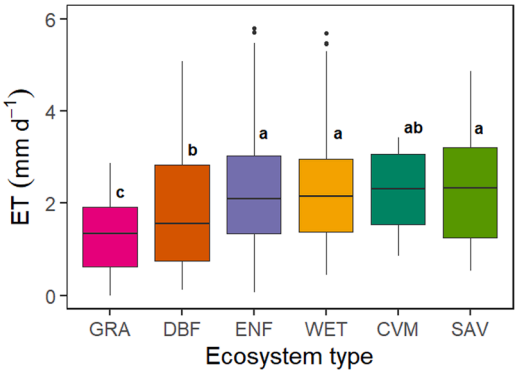

Fig. 6. Variation in monthly ecosystem evapotranspiration (ET) across ecosystem type GRA (Grassland), DBF (Deciduous Broadleaf Forests), CVM (Cropland Vegetation Mosaic), ENF (Evergreen Needleleaf Forests), WET (Wetlands), and SAV (Savannas). Monthly data were used in the analysis. In the boxplots, the thick horizontal line shows the median; the box extends to the upper and lower quartiles; and the thin vertical lines indicate the range. Different letters denote significant differences among ecosystem type ($p < 0.05$).

ratios of up to 1.52. DBF had the lowest ET:P (0.44), while the SAV sites consumed more water than the forest ecosystems (0.82). The PET:P ratio in DBF was also the lowest (0.82), but the PET at SAV was 1.5 times higher than P (1.52). The WET sites at the lower coastal plains in Florida and North Carolina WET sites had a ET:P ratio of 0.73, but the PET:P ratio in Florida's wetlands reached 1.15. However, evaluating ET as affected by P or PET alone is not sufficient to explain ET trends, especially when detecting anomalies. Thus, the need for the Budyko framework to understand better the ET evaporative and dryness indices across ecosystems.

3.3. *Detecting ET anomalies using the Budyko framework*

We determined the site variation in the evaporative index (ET/P) and dryness index (PET/P) using the Budyko framework. In the Budyko space, it showed that ENF had the highest relative evaporative water losses (ET/P), while DBF (i.e., low PET/P) was least sensitive to drought (Fig. 9). Surprisingly, Florida's wetland sites appear to be moving towards water-limited systems (PET/$P > 1.0$).

To determine how our data fit in the two widely used Budyko models, we embedded the mean annual ET data in the Budyko space (Fu, 1981; Zhang et al., 2004, 2001) to describe the relationship between evaporative and dryness indices. We found that these generalized models fit the data well. As expected, the Budyko parameter w of 2.72 developed in this study slightly deviated from the other two models for either forests or grasslands (Fu, 1981; Zhang et al., 2004). However, it appears that the generalized model with a parameter of 2.72 is sufficient to represent the Southeast region as a whole (Fig. 9). In this study, we could not derive ecosystem specific w parameter due to data sample

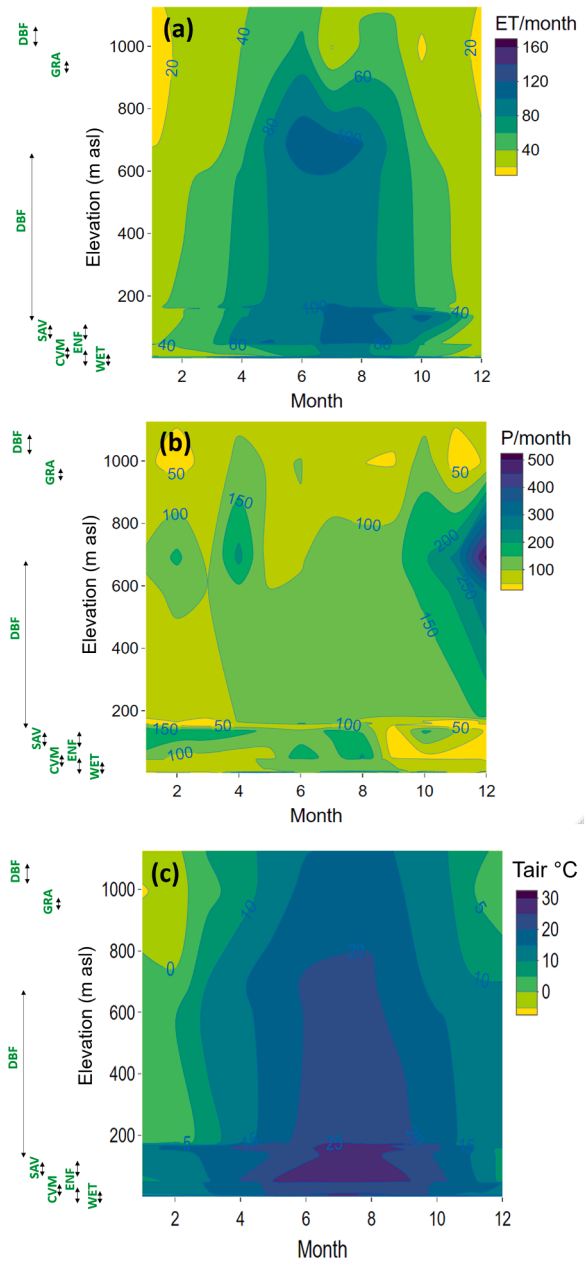

Fig. 7. Contour plots of the seasonal variation in (a) ecosystem evapotranspiration (ET, mm), (b) precipitation (P, mm) and air temperature (Tair, °C) as a function of elevation (m, asl) across different ecosystem types in the U.S. Southeast including GRA (Grasslands), DBF (Deciduous Broadleaf Forests), CVM (Cropland Vegetation Mosaics), ENF (Evergreen Needleleaf Forests), WET (Wetlands), and SAV (Savannas).

limitations.

3.4. Functional response of evapotranspiration to climatic and biological forcings

We used monthly PET, LAI, Rn, VPD, T_{air}, and P as predictor variables to model monthly ET. By lumping all sites together, the GAM modeling revealed that LAI is the best single predictor, explaining 59% of the variation (computation not shown). The combined climate and biological variables explained 78% of the variation in ET (Table 3).

Using only monthly LAI as a predictor variable for ET in the DBF site was enough to explain most of the variation in ET with $R^2 = 0.76$ ($p < 0.05$). In contrast, PET was the sole predictor variable for the CVM site ($R^2 = 0.91$ ($p < 0.01$) (Table 3). Four variables (LAI, PET, P, and T_{air}) were needed to best explain the most change in ET at the ENF sites ($R^2 = 0.79$, $p < 0.001$), with LAI ranked as the best predictor. The best predictor variables for GRA sites were LAI, Rn, and PET ($R^2 = 0.88$, $p < 0.001$), while VPD, Rn, LAI, and PET best explained ET at the SAV sites ($R^2 = 0.88$, $p < 0.001$). At the WET sites, LAI was the primary predictor of ET together with PET and VPD ($R^2 = 0.69$, $p < 0.001$). Overall, LAI was the most limiting factor as it appeared as one of the best predictor variables across all ecosystem types, except in the SAV site. However, P, representing the water availability, was the least limiting factor for ET across ecosystems.

The univariate linear models showed a slightly weaker ET-PET relationship in WET (R^2=0.43, $p < 0.05$, Fig. 10b). However, any increase in PET would significantly increase ET in drier areas, e.g. CVM (R^2=0.91, $p < 0.01$) and SAV (R^2=0.68, $p < 0.01$). LAI was the least limiting factor for the WET site (R^2=0.48, $p < 0.05$, Fig. 10a). The highest correlation between ET and LAI occurred in CVM sites (R^2=0.76, $p < 0.01$). Overall, the ET at all sites was sensitive to LAI and PET (Fig. 10a and b). Precipitation was not a significant factor affecting ET at most sites (R^2=0.01–0.22) (Fig. 10c).

3.5. Comparison of various models using machine learning approaches to predict ET

To further evaluate the combined effects of PET, LAI, and P on ET rates, we developed models using the artificial neural network (ANN), Generalized Additive Model (GAM), Multiple Linear Regression (MLR), and Randon Forest (RF) methods. We used the three main input variables PET, LAI, and P to be comparable with other studies (Fang et al., 2016; Sun et al., 2011a).

Results showed that when the monthly data were pooled across all sites, the modeled ET using ANN, RF, MLR, and GAM explained 84% of the deviation in observed ET. However, when considering each ecosystem type separately, the models explained 82% to 95% of the variations in observed ET. ANN was the best modeling procedure, ranking first to have a good fit between the ANN-model-derived ET and the observed ET, whereas, RF was the second-best-fitting model (Table 4). GAM and MLR fittings were the poorest and were excluded from modeling results in most of the ecosystem types since their

Table 2
Mean annual P, ET and PET across all sites including cropland vegetation mosaic (CVM), deciduous broadleaf forest (DBF), evergreen needleleaf forest (ENF), grassland (GRA), savannas (SAV), and wetland (WET) sites.

Ecosystem	Annual P (mm)			Annual ET (mm)			Annual PET (mm)		
	Mean	Min	Max	Mean	Min	Max	Mean	Min	Max
All	1062	538	1870	774	391	1327	1207	565	1574
CVM	1295	1282	1307	819	759	880	1451	1431	1472
DBF	1256	674	1870	688	574	864	1039	652	1562
ENF	1068	538	1616	796	436	1327	1201	882	1509
GRA	900	791	984	489	391	589	678	565	836
SAV	931	613	1254	828	643	969	1411	1223	1556
WET	1127	813	1372	814	518	1032	1216	859	1574

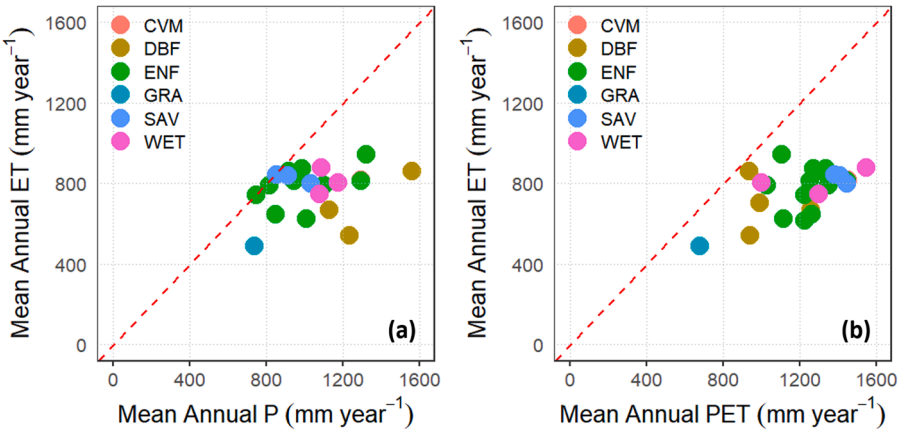

Fig. 8. Patterns of mean annual ET and P (a) and ET and PET (b) across GRA (Grasslands), DBF (Deciduous Broadleaf Forests), CVM (Cropland Vegetation Mosaics), ENF (Evergreen Needleleaf Forests), WET (Wetlands), and SAV (Savannas) ecosystems in the U.S. Southeast.

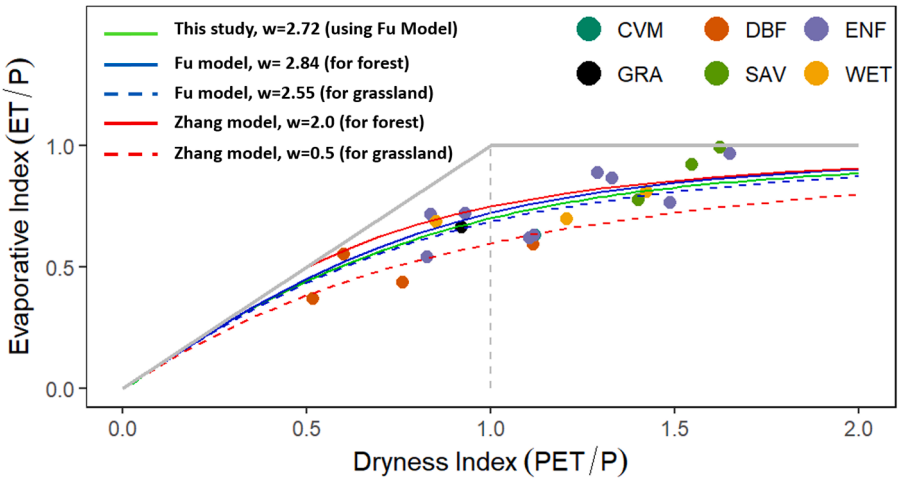

Fig. 9. The Budyko curves derived using the mean annual data of ET, PET, and P across the flux sites in the U.S. Southeast. The thick gray and dashed gray lines show the physical boundaries of the curve where the dryness index (PET/P) increases with the evaporative index (ET/P) over the energy-limited region and where ET/P is independent of PET/P over the water-limited region. Comparison of the Budyko curves derived using the Fu et al., 1981 (blue line), Zhang et al., 2001 (red line), and the model developed in this study by optimizing the w (plant-available water coefficient) to 2.67 (green line). Ecosystem type is denoted by colored circles in each panel as GRA (Grasslands), DBF (Deciduous Broadleaf Forests), CVM (Cropland Vegetation Mosaics), ENF (Evergreen Needleleaf Forests), WET (Wetlands), and SAV (Savannas).

relationship with ET was insignificant. ($p > 0.05$).

4. Discussion

4.1. Variability in biological and climate variables across elevation gradients

The distribution of precipitation and temperature across elevational gradients played an important role in determining water availability, which in turn, influenced ecosystem structure (e.g., biomass) and function (e.g. water yield).

Our study showed that air temperature exhibited higher variability (8.0 °C – 12.9 °C) at high elevation (DBF and GRA sites) compared to lower-elevation sites at CVM, SAV, and WET (17.9 °C – 22.8 °C) ($p <$ 0.05; Supplemental Table 2; Fig. 5 and 7c). This pattern is typical for mountainous areas characterized by complex topography and uneven precipitation and temperature regimes (Amatya et al., 2018; Qin et al., 2009; Sun et al., 2020). The monthly precipitation (74.9 mm month^{-1} – 107.8 mm month^{-1}) and mean air temperature range (8.0 °C – 22.8 °C; Supplemental Table 2, Fig. 7b and c) range followed the patterns from across the Southeast U.S. and the United States (Sun et al., 2011b). Among all the sites, the GRA site represents the low end of the range in P (74.9 mm month^{-1}) and temperature (8.0 °C) (Fig. 7b and c) and other climatic and biological variables (i.e. PET, LAI, Rn, and VPD; Supplemental Table 2). GRA (US-Cav) is located in the Canaan Valley in West Virginia with an elevation of 994 m asl (Meyers, 2016). US-Cav site is an area where trees and shrubs covered less than 10% of the site, and precipitation was the lowest of all sites in this study (74.9 mm month^{-1}, on average) and the lowest PET (56.4 mm month^{-1}, on average, Supplemental Table 2). GRA has the lowest LAI of 1.32 due to the low rainfall ($R^2 = 0.13$) and energy-related climate parameter (e.g., Rn, $R^2 =$ 0.90). However, ENF sites have a precipitation (89.0 mm month^{-1}) and mean temperature (18.2 °C) regime that can support ENF conifer forests where trees remain green all year round, and thus have the highest LAI (4.11) ($p < 0.05$) (Supplemental Table 2). The monthly PET (117.5 mm month^{-1}) that exceeds the monthly rainfall amount (77.5 mm month^{-1}) at SAV is a characteristic of somewhat drier soil-water environment (Supplemental Table 2). A combination of high PET and low rainfall might explain the water stress resulting in a low LAI in water-limited ecosystems (Zeppel et al., 2006).

Table 3
Results of the generalized additive model (GAM) analysis to rank predictor variables (LAI, PET, P, Rn, VPD, and Tair) according to the ability to explain variation in ET. Multiple coefficients of determination, p-values, and AIC were also provided. The smaller the AIC value, the better the model fit. The best-fit predictor model equation for each ecosystem type is also shown. Variables were ranked from highest to lowest based on the order in which they appear in the predictor variables column and the best predictor model result. Monthly data were used in the analysis.

Ecosystem	Response variable	Predictor variables	Multiple R^2	p-value	AIC
ALL	ET ~	LAI	0.59	<0.05	8794
		LAI + PET	0.61	<0.05	8658
		LAI + PET + Tair	0.64	<0.001	8696
		LAI + PET + Tair + *P*	0.7	<0.001	8515
		LAI + PET + Tair + *P* + VPD	0.71	<0.001	8488
		LAI + PET + Tair + *P* + VPD + Rn	0.78	<0.001	8175
CVM	ET ~	PET	0.91	<0.05	116
DBF	ET ~	LAI	0.76	<0.01	353
ENF	ET ~	LAI	0.51	<0.05	2768
		LAI + PET	0.64	<0.01	2691
		LAI + PET + *P*	0.71	<0.001	2677
		LAI + PET + *P* + Tair	0.79	<0.001	2671
GRA	ET ~	LAI	0.66	<0.05	244
		LAI + Rn	0.84	<0.01	236
		LAI + Rn + PET	0.88	<0.001	230
SAV	ET ~	VPD	0.82	<0.001	3075
		VPD + Rn	0.86	<0.001	2541
		VPD + Rn + LAI	0.87	<0.001	2488
		VPD + Rn + LAI + PET	0.88	<0.001	2472
WET	ET ~	LAI	0.48	<0.001	2276
		LAI + PET	0.53	<0.001	2147
		LAI + PET + VPD	0.69	<0.001	2141

Ecosystem	Best Predictor Model	Multiple R^2	*n*
ALL	ET = −4.47 + 8.84 LAI + 0.29 PET + 0.93 Tair + 0.04 P - 0.57 VPD + 0.01 Rn	0.78	1813
CVM	ET = −4.26 + 0.63 PET	0.91	36
DBF	ET = 2.32 + 19.94 LAI	0.76	216
ENF	ET = −12.35 + 10.89 LAI + 0.21 PET + 0.09 *P* + 0.82 Tair	0.79	900
GRA	ET = 10.36 + 11.49 LAI + 0.15 Rn + 0.05 PET	0.88	72
SAV	ET = 7.64 - 2.50 VPD + 0.17 Rn + 13.18 LAI + 0.26 PET	0.88	324
WET	ET = 2.97 + 14.75 LAI + 0.35 PET - 1.72 VPD	0.69	264

4.2. Variation in ET in relation to PET and P across elevation gradients and ecosystems types

At most sites, the monthly ET (40.8 mm month^{-1} – 69.0 month^{-1}) is lower than P (75.0 mm month $^{-1}$ – 107.8 mm month^{-1}) ($p < 0.05$; Supplemental Table 2), indicating that severe water stress is unlikely unless perhaps, during extreme drought events. Our synthesis study indicated that the highest ET rates occur in the summer months (Fig. 7a), as commonly observed in other studies in the humid region (Aguilos et al., 2021a; Amatya et al., 2016b; Aulenbach and Peters, 2018). The 16% excess of PET over P (Supplemental Table 2) suggests that actual ET is down regulated by the biological processes in this humid region.

At the lower elevation sites (SAV, CVM, WET, ENF), the mean seasonal ET rates varied from 66.2 mm month^{-1} to 69.0 mm month^{-1}, and were higher compared to the higher elevation DBF and GRA sites at 40.8 mm month^{-1} and 50.3 mm month^{-1}, respectively ($p < 0.05$, Fig. 7a, Supplemental Table 2). This supports our hypothesis that ET is higher at lower elevation sites regardless of the land cover. The large differences in P between the growing season (125 mm month^{-1}) and the non-growing season (69 mm month^{-1}) (Fig. 7b, seasonal data not shown) at the WET sites did not result in large seasonal differences in ET accounting for about 70% of P (Fig. 7a). This suggests that ET rates are not significantly affected by the amount of P in wetlands, and these wetlands

Table 4
Model comparisons using the Akaike Information Criterion (AIC).

Ecosystem	Deviance Explained	Model Rank	Models	F-value	p-value	AIC
ALL	84%					
		1st	ANN	125.46	<0.001	2019
		2nd	RF	9.65	<0.01	3306
		3rd	MLR	5.33	<0.05	3365
		4th	GAM	0.84	ns	3376
CVM	85%					
		1st	ANN	7.67	<0.01	29
DBF	92%					
		1st	ANN	43.9	<0.001	74
ENF	82%					
		1st	ANN	47.49	<0.001	1086
		2nd	RF	6.21	<0.01	1705
GRA	95%					
		1st	ANN	16.1	<0.001	24
		2nd	RF	3.16	<0.01	138
SAV	90%					
		1st	ANN	154.37	<0.001	323
		2nd	RF	12.46	<0.001	521
		3rd	MLR	6.91	<0.01	608
WET	95%					
		1st	ANN	71.35	<0.001	456
		2nd	GAM	4.18	<0.01	677

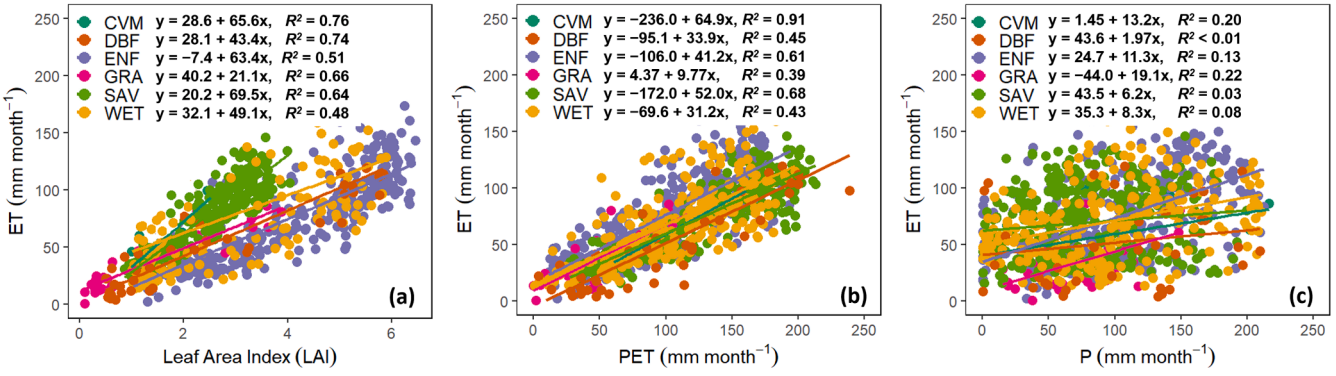

Fig. 10. Relationships between evapotranspiration (ET) and (a) leaf area index (LAI), (b) Priestley-Taylor ET (PET), Evapotranspiration (ET), and Precipitation (P) across ecosystem types in the U.S. Southeast: GRA (Grassland), DBF (Deciduous Broadleaf Forests), CVM (Cropland Vegetation Mosaic), ENF (Evergreen Needleleaf Forests), WET (Wetlands), and SAV (Savannas).

release a consistent amount of water throughout the year.

Lower rainfall slightly impacted ET rates at GRA (61.3 mm month^{-1}) and DBF (108.9 mm month^{-1}) at higher elevations (>600 m asl) during the growing season (May – September), and even more during winter at 47 mm month^{-1} and 23 mm month^{-1}, respectively (Fig. 7a, seasonal data not shown). Low ET rates at these sites may be attributed to factors like lower LAI, temperature, and net radiation received at high elevations. ET is limited by energy in the winter months when precipitation (i.e., snow and rainfall) exceeds atmospheric demand (Sun et al., 2011a). During the non-growing season, ET is reduced due to low temperatures, decreased Rn (Gong et al., 2006), and reduced canopy conductance (Zhang et al., 2016). While our synthesis study suggests that water loss rates from many ecosystems are highest during the growing season, a larger sample size and representation of more vegetation type is needed to fully characterize this process.

On an annual basis, mean P (1062 mm year^{-1}) far exceeded ET (774 mm year^{-1}) rates for most ecosystem types in the study region with occasionally ET>P in dry years (Table 2). Globally, ecosystem ET accounts for almost half of the total water loss from most terrestrial ecosystems (Zhang et al., 2001). In water-limited or semi-arid systems (e.g., savannas, croplands, grasslands, etc.), the percentage of water lost is greater or equal to P (Wang et al., 2011). However, the grassland site (US-Cav) in our study has the lowest ET rates (489 mm year^{-1}) among all ecosystem types (Table 2). Grasslands cover the cool mountains (i.e., lowest PET among all sites) and predominantly comprise shallow clayey soils with low infiltration rates, porosity, and hydraulic conductivity and low storage capacity, thus resulting in lowest ET rates (Buol and Weed, 1991; Markewich et al., 1990). Cropland had the highest PET (1451 mm year^{-1}), which it exceeded P (1295 mm year^{-1}) by 11% (Table 2). The CVM site (US-xDS) is a part of the 12,000-acre Disney Wilderness Preserve that straddles the headwaters of the Everglades ecosystem in Florida (NEON, 2022). This site is seasonally wet and flooded and was used as ranchland, and thus is an open area. The P of lower elevations, ENF and SAV sites (1068 mm year^{-1} and 931 mm year^{-1}, respectively), were also lower than PET (1201 mm year^{-1} and 1411 mm year^{-1}, respectively), suggesting dry conditions. PET at GRA and DBF sites (678 mm year^{-1} and 1039 mm year^{-1}, respectively) was lower than P (900 mm year^{-1} and 1256 mm year^{-1}, respectively) ($P < 0.05$), suggesting more water is transferred to the soil rather than being released to the atmosphere.

4.3. The Budyko framework

The ET, P, and PET relationships have been extensively studied using the Budyko framework (Budyko, 1974; Sposito, 2017; Zhang et al., 2004). Even in a humid region with high precipitation, PET/P still had a large range, indicating large PET at some sites (Fig. 9). The high elevation ecosystems GRA and DBF were energy-limited (PET/$P < 1$), while conifer forests (ENF) and savannas (SAV) on the coastal plain could potentially become water-limited (PET/$P > 1$). When water is not limited, conifer forests (ENF) in warm environments have higher ET than deciduous forests ($p < 0.05$).

An interesting finding from our analysis is that WET sites can become water-limited, possibly due to low P and insufficient surface water drainage from surrounding uplands, especially during summer (Aguilos et al., 2021a, 2020). Unfortunately, our analysis could not fully capture extreme events, such as droughts, due to the limited coverage period of flux measurement. This limitation highlights the need to have local topographic information to evaluate drought effects on ET at the site level. The derived general parameter w (2.72) for the Budyko model in this study does not deviate largely from reported global values (Fu, 1981; Zhang et al., 2004), suggesting that we can potentially use the derived parameter to estimate mean ET for the humid region that is dominated by forests and other vegetations.

4.4. Key environmental controls on ET

Our study showed that energy-related variables (PET, Ta, and Rn), atmospheric dryness (VPD), vegetation structure (LAI), and water supply (P) variables explained 69% to 91% of the monthly variation in ET (Table 3), which aligns with other global studies (Fang et al., 2016; Granata, 2019). Notably, LAI was the most critical limiting factor at most sites, supporting our hypothesis. LAI is the primary control on ET, even in less productive site such as GRA (Nagler et al., 2007). It plays a dominant role in influencing ET rates for different ecosystems, such as deciduous forests, grassland sites, and wetland areas (Zhou et al., 2010) and evergreen forests, (Yang and Zhou, 2011; Zhou et al., 2010). Using LAI as an independent variable allows scaling up ground-based stand--scale ET measurements to the landscape scale using remote sensing approaches (Hwang et al., 2009), especially in dry regions (Nagler et al., 2007). LAI has been shown to be more informative in explaining ET than land cover type (Fang et al., 2016).

For cropland site (CVM), PET was the sole best predictor, indicating a strong response to soil water stress in areas with low soil water content (Stoy et al., 2006). Not surpisingly, P did not strongly influence ET across all sites. This suggests that U.S. Southeast ecosystems rarely experienced severe water stress during the years of this study, especially at forested sites with mature forests having access to deep soil water reserves (Aguilos et al., 2018a).

Our results show that LAI, Rn, and Tair have a more significant influence on ET compared to P. This suggests that ET is primarily controlled by biological factors like canopy structure (LAI) and energy-related parameters, rather than water availability. However, there are other factors not considered here, such as age, disturbance history, land use, soils, vegetation traits, and forest management, which may impact ET and should be explored in future investigations (Aguilos et al., 2014; Komatsu and Kume, 2020; Peel et al., 2010; Williams et al., 2012; Zhang et al., 2001).

4.5. Modeling ET using LAI, PET, and P

While our analysis shows that a series of factors have predictive power for ET at a monthly scale, some climate data (e.g. Rn) were not readily available. Here, we developed simplified yet efficient models using only LAI, PET, and P to predict ET at a regional scale (Fang et al., 2016; Sun et al., 2011a).

Our machine learning algorithms results showed that artificial neural networks (ANN) had the most robust model performance (Table 4). Past research indicated that ANN offers a promising alternative model in hydrological modeling studies (Feng et al., 2017; Kisi, 2008; Stangierski et al., 2019). However, the application of ANN to ET modeling has not been widely explored. Here, the accuracy of all machine learning ET models used here for monthly ET prediction at a regional scale was high, as evidenced by a deviation explaining up to 84% of the variation. The models performed best in DBF, GRA and WET over a wide elevation range, suggesting that future studies would benefit by including latitudinal gradients of diverse ecosystems for better model fitting. However, our data has elevation gaps between ~200 to 600 m and ~600 to 1000 m, which may result in some model uncertainties or lack of representation.

The varying model fittings across different ecosystem types of the U.S. Southeast indicates that no single model equation can adequately capture the spatial variability in ET using the predictors in this analysis. We found a low model fits for CVM (Deviance Explained = 85%) and ENF (DE = 82%), suggesting that even with energy and water-dominated variables (PET and P) coupled with biological component (LAI), the models could not fully account for ET dynamics at these non-water limited sites (Table 4). Additional biological and climatic variables are still needed to address this issue. We found that the model strength of lumped models (developed by pooling all site data together) was inferior (max DE = 84%) to those models developed for each

individual ecosystem (max DE = 95%), suggesting the need to developing ecosystem-specific models, as we hypothesized. Overall, we found no single machine learning algorithm is best for all situations. The performance of the models strongly depends on the size, structure, and quality of available data.

4.6. Limitations and uncertainties

Several challenges and uncertainties are worth mentioning in our analysis of regional monthly ET patterns. One major common uncertainty arises from using eddy covariance flux data, which is measured within a relatively small volume of air but represents the energy and gas exchange integrated over an entire ecosystem over a fixed period of time (usually 30 min to one hour). Additionally, the AmeriFlux database biome representation and land cover classification accuracy pose issues. Many flux sites are located in mature or unmanaged forests (e.g. US-Elm, US-Esm, US-SP1, US-Cwt, US-xGR among others; Supplementary Table 1), potentially underrepresenting recently harvested or young managed forests (e.g. US-NC1, US-NC3, US-HB3) with different ET rates. Moreover, the limited and skewed sample size of the AmeriFlux sites used in this synthesis is biased towards matured forest ecosystems with little disturbance. It is also known that LE data derived from flux towers are also prone to measurement errors related to surface energy balance, 3-D wind measurements, instrument failures, and gap-filling techniques (Leuning et al., 2012; Nakai and Shimoyama, 2012; Shao et al., 2015). Our WET sites also represent contrasting water regimes, especially at the wetland sites. US-NC4, a bottomland hardwood forested wetland forest in North Carolina is energy-limited (Fig. 9), while the other two (US-Esm and US-Elm) in Florida are water-limited wetlands. This can lead to a significant error in ET estimation over this WET ecosystem when data from such disparate sites are aggregated.

Another limitation of our analysis is that we did not account for extreme conditions such as flooding, drought, and forest fire. Future studies should address this to improve water resource management decision-making during extreme events (Nagler et al., 2007). MODIS-derived LAI is shown to be overestimated, especially in a multi-layer structured ecosystem (Cohen et al., 2006). MODIS LAI fluctuated unrealistically, and vegetation misclassification increased the errors in estimating LAI (Fang et al., 2016). Additionally, MODIS LAI has a very coarse spatial resolution (500 m) which has been shown to be inadequate for the U.S. Southeast (Blinn et al., 2019). These errors can be reduced by using Landsat Imagery with higher spatial resolution.

4.7. Implications

Many researchers have primarily focused on the supply side of the water availability (e.g., rainfall, soil water content, groundwater), while largely overlooking the demand side (e.g. ET) (Fisher et al., 2017). Understanding both aspects, especially ET, which historically has been challenging to quantify and scale, is crucial, particularly with the increasing atmospheric water demand driven by climate change and management practices. A holistic approach in assessing the water balance is important for proper water resources management and understanding vegetation stress responses.

In the context of global climate change, our energy-limited environments ($PET/P < 1$) e.g., GRA and DBF, may be more positively and significantly affected by global warming (Figs. 8 and 9). Rising air temperature and VPD increase atmospheric demand, and climate-induced changes are impacting vegetation dynamics, productivity, and species distributions, influencing carbon and water cycles. However, our lower elevation sites that are slightly water-limited environments ($PET/P > 1$) maybe negatively affected in a future warmer climate due to predicted water stress. Thus, any reduction in PET or decline in P could push lower elevation ecosystems to either reduce productivity or fundamentally change in species distribution and prevalence. Thus, continuous monitoring of P and PET trends is crucial for future ecosystem management to enhance ecosystem resilience to the changing climate.

During the period of this study, P was relatively uniformly distributed across the study region. Lower ET losses of water from P during the non-growing season could help in soil water recharge to meet the water demands during the growing season. Disruption of this pattern due to climate change substantially impacts water use, thus affecting ecosystem sustainability and provisioning of ecosystem services to society. As suggested by our synthesis study, decreased P coupled with increasing temperature during the non-growing season could affect ENF and GRA sites with high water consumption in summer (70%−82% of P) and even more severely for the SAV sites with even higher ET water losses (116%). Under such conditions, savanna vegetation might transition into a more degraded ecosystem. Similarly, ET of croplands and conifer plantations exceeded more than 50% of P, potentially compromising stand development This low resilience to future conditions of decreased water availability and higher atmospheric demand could compromise other ecosystem functions, such as productivity, carbon storage, and biodiversity.

5. Conclusions

We present a multi-ecosystem regional synthesis study that elucidates the relationships among between the ecosystem water loss through ET, water and energy availability, and vegetation dynamics. Our findings indicate that water availability may not be the main limiting factor of ET in the humid southeastern U.S. region that is generally 'energy limited'. Monthly and annual ET in the Southeast can be reliably estimated by atmospheric demand alone without, considering precipitation. In addition to energy availability, LAI is a strong control of seasonal ET, suggesting that the vegetation management can modify the hydrology of the study region, The models derived from this study provide a tool to manage ecosystem water balance for sustaining ecosystem functions in a changing environment.

Estimating ecosystem ET at a large scale remains challenging due to incomplete spatial and temporal data coverage, and incomplete representation of diverse ecosystems, physiographic settings and vegetation characteristics including understory vegetation and management practices. Thus, there is a need to expand the network of eddy covariance flux measurements to focus on ecosystems less represented in the current Ameriflux network, such as riparian forests, shrublands, grasslands, savannas, or wetlands sites, especially in highly-disturbed areas (i.e., urban areas) and under various forest management practices (i.e., prescribed burning). Despite the limitations and uncertainties of currently available data, this study provides the template for modeling frameworks, and offers some practical models that can be applied with readily available data to natural water resource management at local or regional scales. Additionally, the ET models are needed to be evaluated against independent data sources such as gaged watersheds and ET estimated from remote sensing.

CRediT authorship contribution statement

Maricar Aguilos: Writing – original draft, Visualization, Methodology, Investigation, Formal analysis, Data curation, Conceptualization. **Ge Sun:** Writing – review & editing, Supervision, Project administration, Methodology, Formal analysis, Conceptualization. **Ning Liu:** Writing – review & editing, Software, Formal analysis, Data curation. **Yulong Zhang:** Writing – review & editing. **Gregory Starr:** Writing – review & editing, Investigation, Data curation. **Andrew Christopher Oishi:** Writing – review & editing, Validation, Investigation, Data curation. **Thomas L O'Halloran:** Writing – review & editing, Validation, Resources, Investigation, Data curation. **Jeremy Forsythe:** Writing – review & editing, Investigation, Data curation. **Jingfeng Wang:** Writing – review & editing, Investigation, Data curation. **Modi Zhu:** Writing – review & editing, Investigation, Data curation. **Devendra Amatya:**

Writing – review & editing. **Benju Baniya:** Writing – review & editing, Software, Data curation. **Steve McNulty:** Writing – review & editing, Supervision, Resources, Project administration, Investigation, Funding acquisition, Conceptualization. **Asko Noormets:** Writing – review & editing, Supervision, Resources, Project administration, Methodology, Investigation, Funding acquisition, Data curation, Conceptualization. **John King:** Writing – review & editing, Supervision, Resources, Project administration, Methodology, Investigation, Funding acquisition, Conceptualization.

Declaration of competing interest

The authors declare that they have no known competing financial interests or personal relationships that could have appeared to influence the work reported in this paper.

Data availability

The authors do not have permission to share data.

Acknowledgement

Primary funding was provided by the USDA NIFA (Multi-agency A.5 Carbon Cycle Science Program) award 2014–67003–22068. Additional funding was provided by the DOE NICCR award 08-SC–NICCR-1072, the USDA Forest Service award 13-JV-11330110–081 and 21-JV-11330180–052, and the DOE LBNL award DE-AC02–05CH11231.

Supplementary materials

Supplementary material associated with this article can be found, in the online version, at doi:10.1016/j.agrformet.2024.109960.

References

Abdullah, S.S., Malek, M.A., Abdullah, N.S., Kisi, O., Yap, K.S., 2015. Extreme Learning Machines: a new approach for prediction of reference evapotranspiration. J. Hydrol. 527, 184–195. https://doi.org/10.1016/j.jhydrol.2015.04.073.

Acharya, S., Kaplan, D.A., McLaughlin, D.L., Cohen, M.J., 2022. In-Situ quantification and prediction of water yield from Southern US pine forests. Water Resour. Res. 58, 1–17. https://doi.org/10.1029/2021WR031020.

Adnan, S., Ullah, K., Ahmed, R., 2020. Variability in meteorological parameters and their impact on evapotranspiration in a humid zone of Pakistan. Meteorol. Appl. 27, 1–10. https://doi.org/10.1002/met.1859.

Aguilos, M., Hérault, B., Burban, B., Wagner, F., Bonal, D., 2018a. What drives long-term variations in carbon flux and balance in a tropical rainforest in French Guiana? Agric. For. Meteorol. 253–254, 114–123. https://doi.org/10.1016/j.agrformet.2018.02.009.

Aguilos, M., Mitra, B., Noormets, A., Minick, K., Prajapati, P., Gavazzi, M., Sun, G., McNulty, S., Li, X., Domec, J.C.J.-C., Miao, G., King, J., 2020. Long-term carbon flux and balance in managed and natural coastal forested wetlands of the Southeastern USA. Agric. For. Meteorol. 288–289. https://doi.org/10.1016/j.agrformet.2020.108022.

Aguilos, M., Stahl, C., Burban, B., Hérault, B., Courtois, E., Coste, S., Wagner, F., Ziegler, C., Takagi, K., Bonal, D., 2018b. Interannual and seasonal variations in ecosystem transpiration and water use efficiency in a tropical rainforest. Forests 10. https://doi.org/10.3390/f10010014.

Aguilos, M., Sun, G., Noormets, A., Domec, J.C., McNulty, S., Gavazzi, M., Minick, K., Mitra, B., Prajapati, P., Yang, Y., King, J., 2021a. Effects of land-use change and drought on decadal evapotranspiration and water balance of natural and managed forested wetlands along the southeastern US lower coastal plain. Agric. For. Meteorol. 303 https://doi.org/10.1016/j.agrformet.2021.108381.

Aguilos, M., Sun, G., Noormets, A., Domec, J.C., McNulty, S., Gavazzi, M., Prajapati, P., Minick, K.J., Mitra, B., King, J., 2021b. Ecosystem productivity and evapotranspiration are tightly coupled in loblolly pine (Pinus taeda l.) plantations along the coastal plain of the southeastern U.S. Forests 12. https://doi.org/10.3390/f12081123.

Aguilos, M., Takagi, K., Liang, N., Ueyama, M., Fukuzawa, K., Nomura, M., Kishida, O., Fukazawa, T., Takahashi, H., Kotsuka, C., Sakai, R., Ito, K., Watanabe, Y., Fujinuma, Y., Takahashi, Y., Murayama, T., Saigusa, N., Sasa, K., 2014. Dynamics of ecosystem carbon balance recovering from a clear-cutting in a cool-temperate forest. Agric. For. Meteorol. 197, 26–39. https://doi.org/10.1016/j.agrformet.2014.06.002.

Aguilos, M., Warr, I., Irving, M., Gregg, O., Grady, S., Peele, T., Noormets, A., Sun, G., Liu, N., McNulty, S., Pettay, F., Bhattacharya, S., Penney, S., Kerrigan, M., Yang, L., Mitra, B., Prajapati, P., Minick, K., King, J., 2022. The unabated atmospheric carbon losses in a drowning wetland forest of North Carolina: a point of no return? Forests 13, 1–19. https://doi.org/10.3390/f13081264.

Amatya, D., Irmak, S., Gowda, P., Sun, G., Nettles, J., Douglas-Mankin, K., 2016a. Ecosystem evapotranspiration: challenges in measurements, estimates, and modeling. Trans. ASABE 59, 555–560. https://doi.org/10.13031/trans.59.11808.

Amatya, D., Muwamba, A., Panda, S., Callahan, T., Harder, S., Pellett, A., 2018. Assessment of spatial and temporal variation of potential evapotranspiration estimated by four methods for South Carolina 5, 3–24.

Amatya, D., Tian, S., Dai, Z., Sun, G., 2016b. Long-term potential and actual evapotranspiration of two different forests on the Atlantic coastal plain. Trans. ASABE 59, 647–660. https://doi.org/10.13031/trans.59.11141.

Anapalli, S.S., Fisher, D.K., Reddy, K.N., Wagle, P., Gowda, P.H., Sui, R., 2018. Quantifying soybean evapotranspiration using an eddy covariance approach. Agric. Water Manag. 209, 228–239. https://doi.org/10.1016/j.agwat.2018.07.023.

Aulenbach, B.T., Peters, N.E., 2018. Quantifying climate-related interactions in shallow and deep storage and evapotranspiration in a forested, seasonally water-limited watershed in the Southeastern United States. Water Resour. Res. 54, 3037–3061. https://doi.org/10.1002/2017WR020964.

Barton, K., 2022. Package ' MuMIn ' Version 1.46.0. R Packag.

Bhattarai, N., Wagle, P., 2021. Recent advances in remote sensing of evapotranspiration. Remote Sens 13, 1–5. https://doi.org/10.3390/rs13214260.

Blinn, C.E., House, M.N., Wynne, R.H., Thomas, V.A., Fox, T.R., Sumnall, M., 2019. Landsat 8 based leaf area index estimation in loblolly pine plantations. Forests 10, 1–18. https://doi.org/10.3390/f10030222.

Budyko, M.I., 1974. Climate and Life. Academic Press, New York.

Buol, S.W., Weed, S.B., 1991. Saprolite-soil transformations in the Piedmont and mountains of North Carolina. Geoderma 51, 15–28. https://doi.org/10.1016/0016-7061(91)90064-Z.

Burnham, K.P., Anderson, D.R., Huyvaert, K.P., 2011. AIC model selection and multimodel inference in behavioral ecology: some background, observations, and comparisons. Behav. Ecol. Sociobiol. 65, 23–35. https://doi.org/10.1007/s00265-010-1029-6.

Caldwell, P.V., Miniat, C.F., Elliott, K.J., Swank, W.T., Brantley, S.T., Laseter, S.H., 2016. Declining water yield from forested mountain watersheds in response to climate change and forest mesophication. Glob. Chang. Biol. 22, 2997–3012. https://doi.org/10.1111/gcb.13309.

Chai, R., Sun, S., Chen, H., Zhou, S., 2018. Changes in reference evapotranspiration over China during 1960–2012: attributions and relationships with atmospheric circulation. Hydrol. Process. 32, 3032–3048. https://doi.org/10.1002/hyp.13252.

Chen, H., Huang, J.J., McBean, E., 2020. Partitioning of daily evapotranspiration using a modified shuttleworth-wallace model, random Forest and support vector regression, for a cabbage farmland. Agric. Water Manag. 228, 105923 https://doi.org/10.1016/j.agwat.2019.105923.

Chen, J.M., Liu, J., 2020. Evolution of evapotranspiration models using thermal and shortwave remote sensing data. Remote Sens. Environ. 237, 111594 https://doi.org/10.1016/j.rse.2019.111594.

Chen, X., Sivapalan, M., 2020. Hydrological basis of the Budyko curve: data-guided exploration of the mediating role of soil moisture. Water Resour. Res. 56, 1–15. https://doi.org/10.1029/2020WR028221.

Cohen, W.B., Maiersperger, T.K., Turner, D.P., Ritts, W.D., Pflugmacher, D., Kennedy, R. E., Kirschbaum, A., Running, S.W., Costa, M., Gower, S.T., 2006. MODIS land cover and LAI collection 4 product quality across nine sites in the western hemisphere. IEEE Trans. Geosci. Remote Sens. 44, 1843–1857. https://doi.org/10.1109/TGRS.2006.876026.

Engström, J., Praskivicz, S., Bearden, B., Moradkhani, H., 2021. Decreasing water resources in Southeastern U.S. as observed by the GRACE satellites. Water Policy 23, 1017–1029. https://doi.org/10.2166/wp.2021.039.

Fang, Y., Sun, G., Caldwell, P., Mcnulty, S.G., Noormets, A., Domec, J.C., King, J., Zhang, Z., Zhang, X., Lin, G., Zhou, G., Xiao, J., Chen, J., 2016. Monthly land cover-specific evapotranspiration models derived from global eddy flux measurements and remote sensing data. Ecohydrology 9, 248–266. https://doi.org/10.1002/eco.1629.

Feng, X.M., Sun, G., Fu, B.J., Su, C.H., Liu, Y., Lamparski, H., 2012. Regional effects of vegetation restoration on water yield across the Loess Plateau. China. Hydrol. Earth Syst. Sci. 16, 2617–2628. https://doi.org/10.5194/hess-16-2617-2012.

Feng, Y., Peng, Y., Cui, N., Gong, D., Zhang, K., 2017. Modeling reference evapotranspiration using extreme learning machine and generalized regression neural network only with temperature data. Comput. Electron. Agric. 136, 71–78. https://doi.org/10.1016/j.compag.2017.01.027.

Fisher, J.B., Melton, F., Middleton, E., Hain, C., Anderson, M., Allen, R., McCabe, M.F., Hook, S., Baldocchi, D., Townsend, P.A., Kilic, A., Tu, K., Miralles, D.D., Perret, J., Lagouarde, J.P., Waliser, D., Purdy, A.J., French, A., Schimel, D., Famiglietti, J.S., Stephens, G., Wood, E.F., 2017. The future of evapotranspiration: global requirements for ecosystem functioning, carbon and climate feedbacks, agricultural management, and water resources. Water Resour. Res. 53, 2618–2626. https://doi.org/10.1002/2016WR020175.

Fritsch, S., Guenther, F., Wright, M., Suling, M., Mueller, S., 2019. Training of neural networks: package "neuralnet".

Fu, B..P., 1981. On the calculation of the evaporation from land surface (in Chinese), Scientia Atmospherica Sinica, 5, 23–31. Sci. Atmos. Sin. 23–31.

Gholz, H.L., Clark, K.L., 2002. Energy Exchange Across a Chronosequence of Slash Pine Forests in Florida. Agricultural and Forest Meteorology.

Gong, L., Xu, C.yu, Chen, D., Halldin, S., Chen, Y.D., 2006. Sensitivity of the penman-monteith reference evapotranspiration to key climatic variables in the Changjiang

(Yangtze River) basin. J. Hydrol. 329, 620–629. https://doi.org/10.1016/j.jhydrol.2006.03.027.
Granata, F., 2019. Evapotranspiration evaluation models based on machine learning algorithms—a comparative study. Agric. Water Manag. 217, 303–315. https://doi.org/10.1016/j.agwat.2019.03.015.
Hu, X.zhen, Long, H.xia, Ding, C.jiang, Gao, S.juan, Hou, R., zhen Hu, X., xia Long, H., jiang Ding, C., juan Gao, S., Hou, R., 2020. Using random forest algorithm to predict super-secondary structure in proteins. J. Supercomput. 76, 3199–3210. https://doi.org/10.1007/s11227-018-2531-2.
Hwang, T., Band, L., Hales, T.C., 2009. Ecosystem processes at the watershed scale: extending optimality theory from plot to catchment. Water Resour. Res. 45, 1–20. https://doi.org/10.1029/2009WR007775.
Kirschbaum, M.U.F.F., 2017. Assessing the merits of bioenergy by estimating marginal climate-change impacts. Int. J. Life Cycle Assess. 22, 841–852. https://doi.org/10.1007/s11367-016-1196-4.
Kisi, O., 2008. The potential of different ANN techniques in evapotranspiration modelling. Hydrol. Process. 22, 2449–2460. https://doi.org/10.1002/hyp.6837.
Komatsu, H., Kume, T., 2020. Modeling of evapotranspiration changes with forest management practices: a genealogical review. J. Hydrol. 585, 124835 https://doi.org/10.1016/j.jhydrol.2020.124835.
Leuning, R., van Gorsel, E., Massman, W.J., Isaac, P.R., 2012. Reflections on the surface energy imbalance problem. Agric. For. Meteorol. 156, 65–74. https://doi.org/10.1016/j.agrformet.2011.12.002.
Liaw, A., Wiener, M., 2002. Classification and Regression by randomForest. R News 2, 18–22.
Ma, Q., Bales, R.C., Rungee, J., Conklin, M.H., Collins, B.M., Goulden, M.L., 2020. Wildfire controls on evapotranspiration in California's Sierra Nevada. J. Hydrol. 590, 125364 https://doi.org/10.1016/j.jhydrol.2020.125364.
Mackay, D.S., Ewers, B.E., Cook, B.D., Davis, K.J., 2007. Environmental drivers of evapotranspiration in a shrub wetland and an upland forest in northern Wisconsin. Water Resour. Res. 43, 1–14. https://doi.org/10.1029/2006WR005149.
Malone, R.W., Yagow, G., Baffaut, C., Gitau, M.W., Qi, Z., Amatya, D.M., Parajuli, P.B., Bonta, J.V., Green, T.R., 2015. Parameterization guidelines and considerations for hydrologic models. Trans. ASABE 58, 1681–1703. https://doi.org/10.13031/trans.58.10709.
Markewich, H.W., Pavich, M.J., Buell, G.R., 1990. Contrasting soils and landscapes of the Piedmont and Coastal Plain, eastern United States. Geomorphology 3, 417–447. https://doi.org/10.1016/0169-555X(90)90015-I.
Markos, N., Radoglou, K., 2023. Environmental Drivers of Gross Primary Production and Evapotranspiration at a Robinia pseudoacacia L. Restoration Plantation.
Markwitz, C., Siebicke, L., 2019. Low-cost eddy covariance: a case study of evapotranspiration over agroforestry in Germany. Atmos. Meas. Tech. 12, 4677–4696. https://doi.org/10.5194/amt-12-4677-2019.
Mclaughlin, D.L., Kaplan, D.A., Cohen, M.J., 2013. Managing forests for increased regional water yield in the southeastern U.S. coastal plain. J. Am. Water Resour. Assoc. 49, 953–965. https://doi.org/10.1111/jawr.12073.
McQuillan, K.A., Hwang, T., Martin, K.L., 2022. Extended growing seasons and decreases in hydrologic connectivity indicate increasing water stress in humid, temperate forests. SSRN Electron. J. 338, 109525 https://doi.org/10.2139/ssrn.4272101.
Mehdizadeh, S., 2018. Estimation of daily reference evapotranspiration (ETo) using artificial intelligence methods: offering a new approach for lagged ETo data-based modeling. J. Hydrol. 559, 794–812. https://doi.org/10.1016/j.jhydrol.2018.02.060.
Meyers, T., 2016. AmeriFlux BASE US-CaV Canaan Valley, Ver. 2-1, AmeriFlux AMP, (Dataset). https://doi.org/10.17190/AMF/1246042.
Montieth, J.L., 1965. Evaporation and environment. Symp. Soc. Exp. Biol. 19, 205–234.
Mu, Q., Zhao, M., Running, S.W., 2011. Improvements to a MODIS global terrestrial evapotranspiration algorithm. Remote Sens. Environ. 115, 1781–1800. https://doi.org/10.1016/j.rse.2011.02.019.
Nagler, P.L., Glenn, E.P., Kim, H., Emmerich, W., Scott, R.L., Huxman, T.E., Huete, A.R., 2007. Relationship between evapotranspiration and precipitation pulses in a semiarid rangeland estimated by moisture flux towers and MODIS vegetation indices. J. Arid Environ. 70, 443–462. https://doi.org/10.1016/j.jaridenv.2006.12.026.
Nakai, T., Shimoyama, K., 2012. Ultrasonic anemometer angle of attack errors under turbulent conditions. Agric. For. Meteorol. 162–163, 14–26. https://doi.org/10.1016/j.agrformet.2012.04.004.
Negm, A., Minacapilli, M., Provenzano, G., 2018. Downscaling of American National Aeronautics and Space Administration (NASA) daily air temperature in Sicily, Italy, and effects on crop reference evapotranspiration. Agric. Water Manag. 209, 151–162. https://doi.org/10.1016/j.agwat.2018.07.016.
Nema, M.K., Khare, D., Chandniha, S.K., 2017. Application of artificial intelligence to estimate the reference evapotranspiration in sub-humid Doon valley. Appl. Water Sci. 7, 3903–3910. https://doi.org/10.1007/s13201-017-0543-3.
NEON, 2022. NEON (National Ecological Observatory Network), 2022. AmeriFlux BASE US-xDS NEON Disney Wilderness Preserve (DSNY), Ver. 5-5, AmeriFlux AMP, (Dataset). https://doi.org/10.17190/AMF/1671895, 10.17190/AMF/1671895.
Nobrega, R., Guzha, A.C., Torres, G.N., Kovacs, K., Lamparter, G., Amorim, R.S.S., Couto, E., Gerold, G., 2017. Effects of conversion of native cerrado vegetation to pasture on soil hydro-physical properties, evapotranspiration and streamflow on the Amazonian agricultural frontier. PLoS ONE 12, 1–22. https://doi.org/10.17605/OSF.IO/UBKYD.
Noormets, A., Gavazzi, M.J., McNulty, S.G., Domec, J.C., Sun, G., King, J.S., Chen, J., 2010. Response of carbon fluxes to drought in a coastal plain loblolly pine forest. Glob. Chang. Biol. 16, 272–287. https://doi.org/10.1111/j.1365-2486.2009.01928.x.
Noormets, A., McNulty, S.G., DeForest, J.L., Sun, G., Li, Q., Chen, J., 2008. Drought during canopy development has lasting effect on annual carbon balance in a deciduous temperate forest. New Phytol 179, 818–828. https://doi.org/10.1111/j.1469-8137.2008.02501.x.
Oishi, A.C., Miniat, C.F., Novick, K.A., Brantley, S.T., Vose, J.M., Walker, J.T., 2018. Warmer temperatures reduce net carbon uptake, but do not affect water use, in a mature southern Appalachian forest. Agric. For. Meteorol. 252, 269–282. https://doi.org/10.1016/j.agrformet.2018.01.011.
Paul-Limoges, E., Black, T.A., Christen, A., Nesic, Z., Jassal, R.S., 2015. Effect of clearcut harvesting on the carbon balance of a Douglas-fir forest. Agric. For. Meteorol. 203, 30–42. https://doi.org/10.1016/j.agrformet.2014.12.010.
Peel, M.C., McMahon, T.A., Finlayson, B.L., 2010. Vegetation impact on mean annual evapotranspiration at a global catchment scale. Water Resour. Res. 46, 1–16. https://doi.org/10.1029/2009WR008233.
Ponraj, A.S., Vigneswaran, T., 2020. Daily evapotranspiration prediction using gradient boost regression model for irrigation planning. J. Supercomput. 76, 5732–5744. https://doi.org/10.1007/s11227-019-02965-9.
Priestley, C.H.B., Taylor, R.J., 1972. On the assessment of surface heat flux and evaporation using large-scale parameters. Mon. Weather Rev. 100, 81–92. https://doi.org/10.1175/1520-0493(1972)100<0081:otaosh>2.3.co;2.
Qin, J., Yang, K., Liang, S., Guo, X., 2009. The altitudinal dependence of recent rapid warming over the Tibetan Plateau. Clim. Change 97, 321–327. https://doi.org/10.1007/s10584-009-9733-9.
Ringgaard, R., Herbst, M., Friborg, T., 2012. Partitioning of forest evapotranspiration: the impact of edge effects and canopy structure. Agric. For. Meteorol. 166–167, 86–97. https://doi.org/10.1016/j.agrformet.2012.07.001.
Shao, J., Zhou, X., Luo, Y., Li, B., Aurela, M., Billesbach, D., Blanken, P.D., Bracho, R., Chen, J., Fischer, M., Fu, Y., Gu, L., Han, S., He, Y., Kolb, T., Li, Y., Nagy, Z., Niu, S., Oechel, W.C., Pinter, K., Shi, P., Suyker, A., Torn, M., Varlagin, A., Wang, H., Yan, J., Yu, G., Zhang, J., 2015. Biotic and climatic controls on interannual variability in carbon fluxes across terrestrial ecosystems. Agric. For. Meteorol. 205, 11–22. https://doi.org/10.1016/j.agrformet.2015.02.007.
Soloway, A.D., Amiro, B.D., Dunn, A.L., Wofsy, S.C., 2017. Carbon neutral or a sink? Uncertainty caused by gap-filling long-term flux measurements for an old-growth boreal black spruce forest. Agric. For. Meteorol. 233, 110–121. https://doi.org/10.1016/j.agrformet.2016.11.005.
Soubie, R., Heinesch, B., Granier, A., Aubinet, M., Vincke, C., 2016. Evapotranspiration assessment of a mixed temperate forest by four methods: eddy covariance, soil water budget, analytical and model. Agric. For. Meteorol. 228–229, 191–204. https://doi.org/10.1016/j.agrformet.2016.07.001.
Sposito, G., 2017. Understanding the budyko equation. Water (Switzerland) 9. https://doi.org/10.3390/w9040236.
Stangierski, J., Weiss, D., Kaczmarek, A., 2019. Multiple regression models and Artificial Neural Network (ANN) as prediction tools of changes in overall quality during the storage of spreadable processed Gouda cheese. Eur. Food Res. Technol. 245, 2539–2547. https://doi.org/10.1007/s00217-019-03369-y.
Stoy, P.C., Katul, G.G., Siqueira, M.B.S.S., Juang, J.Y., Novick, K.A., Mccarthy, H.R., Oishi, A.C., Uebelherr, J.M., Kim, H.S., Oren, R., 2006. Separating the effects of climate and vegetation on evapotranspiration along a successional chronosequence in the southeastern US. Glob. Chang. Biol. 12, 2115–2135. https://doi.org/10.1111/j.1365-2486.2006.01244.x.
Sun, G., Alstad, K., Chen, J., Chen, S., Ford, C.R., Lin, G., Liu, C., Lu, N., Mcnulty, S.G., Miao, H., Noormets, A., Vose, J.M., Wilske, B., Zeppel, M., Zhang, Y., Zhang, Z., 2011a. A general predictive model for estimating monthly ecosystem evapotranspiration. Ecohydrology 4, 245–255. https://doi.org/10.1002/eco.194.
Sun, G., Caldwell, P., Noormets, A., McNulty, S.G., Cohen, E., Moore Myers, J., Domec, J.- C., Treasure, E., Mu, Q., Xiao, J., John, R., Chen, J., 2011b. Upscaling key ecosystem functions across the conterminous United States by a water-centric ecosystem model. J. Geophys. Res. 116, 1–16. https://doi.org/10.1029/2010jg001573.
Sun, G., Domec, J.C., Amatya, D.M., 2016. Forest evapotranspiration: measurement and modelling at multiple scales. For. Hydrol. Process. Manag. Assess. 32–50 https://doi.org/10.1079/9781780646602.0032.
Sun, G., Hallema, D., Asbjornsen, H., 2017. Ecohydrological processes and ecosystem services in the Anthropocene: a review. Ecol. Process. 6 https://doi.org/10.1186/s13717-017-0104-6.
Sun, G., McNulty, S.G., Moore Myers, J.A., Cohen, E.C., 2008. Impacts of multiple stresses on water demand and supply across the southeastern United States. J. Am. Water Resour. Assoc. 44, 1441–1457. https://doi.org/10.1111/j.1752-1688.2008.00250.x.
Sun, G., Noormets, A., Gavazzi, M.J., McNulty, S.G., Chen, J., Domec, J.C., King, J.S., Amatya, D.M., Skaggs, R.W., 2010. Energy and water balance of two contrasting loblolly pine plantations on the lower coastal plain of North Carolina. USA. For. Ecol. Manage. 259, 1299–1310. https://doi.org/10.1016/j.foreco.2009.09.016.
Sun, J., Wang, G., Sun, X., Lin, S., Hu, Z., Huang, K., 2020. Elevation-dependent changes in reference evapotranspiration due to climate change. Hydrol. Process. 34, 5580–5594. https://doi.org/10.1002/hyp.13978.
Uyanık, G.K., Güler, N., 2013. A study on multiple linear regression analysis. Procedia - Soc. Behav. Sci. 106, 234–240. https://doi.org/10.1016/j.sbspro.2013.12.027.
Wang, Y., Yu, P., Feger, K.H., Wei, X., Sun, G., Bonell, M., Xiong, W., Zhang, S., Xu, X., 2011. Annual runoff and evapotranspiration of forestlands and non-forestlands in selected basins of the Loess Plateau of China. Ecohydrology 4, 277–287. https://doi.org/10.1002/eco.215.
Williams, C.A., Reichstein, M., Buchmann, N., Baldocchi, D., Beer, C., Schwalm, C., Wohlfahrt, G., Hasler, N., Bernhofer, C., Foken, T., Papale, D., Schymanski, S., Schaefer, K., 2012. Climate and vegetation controls on the surface water balance:

synthesis of evapotranspiration measured across a global network of flux towers. Water Resour. Res. 48, 1–13. https://doi.org/10.1029/2011WR011586.
Xu, C.Y., Singh, V.P., 2005. Evaluation of three complementary relationship evapotranspiration models by water balance approach to estimate actual regional evapotranspiration in different climatic regions. J. Hydrol. 308, 105–121. https://doi.org/10.1016/j.jhydrol.2004.10.024.
Xu, C.Y., Singh, V.P., 2004. Review on regional water resources assessment models under stationary and changing climate. Water Resour. Manag. 18, 591–612. https://doi.org/10.1007/s11269-004-9130-0.
Xu, S., Yu, Z., Yang, C., Ji, X., Zhang, K., 2018. Trends in evapotranspiration and their responses to climate change and vegetation greening over the upper reaches of the Yellow River Basin. Agric. For. Meteorol. 263, 118–129. https://doi.org/10.1016/j.agrformet.2018.08.010.
Xuanxuan, Z., 2018. Multivariate linear regression analysis on online image study for IoT. Cogn. Syst. Res. 52, 312–316. https://doi.org/10.1016/j.cogsys.2018.07.014.
Yanagihara, H., Kamo, K., Tonda, T., 2023. Second-order bias-corrected AIC in multivariate normal linear models under non-normality. Can. J. Stat. 39, 126–146.
Yang, F., Zhou, G., 2011. Characteristics and modeling of evapotranspiration over a temperate desert steppe in Inner Mongolia. China. J. Hydrol. 396, 139–147. https://doi.org/10.1016/j.jhydrol.2010.11.001.
Yang, Y., Anderson, M.C., Gao, F., Hain, C.R., Semmens, K.A., Kustas, W.P., Noormets, A., Wynne, R.H., Thomas, V.A., Sun, G., 2017. Daily Landsat-scale evapotranspiration estimation over a forested landscape in North Carolina, USA, using multi-satellite data fusion. Hydrol. Earth Syst. Sci. 21, 1017–1037. https://doi.org/10.5194/hess-21-1017-2017.
Yaseen, Z.M., Sulaiman, S.O., Deo, R.C., Chau, K.W., 2019. An enhanced extreme learning machine model for river flow forecasting: state-of-the-art, practical applications in water resource engineering area and future research direction. J. Hydrol. 569, 387–408. https://doi.org/10.1016/j.jhydrol.2018.11.069.
Zeppel, M.J.B.B., Yunusa, I.A.M.M., Eamus, D., 2006. Daily, seasonal and annual patterns of transpiration from a stand of remnant vegetation dominated by a coniferous Callitris species and a broad-leaved Eucalyptus species. Physiol. Plant. 127, 413–422. https://doi.org/10.1111/j.1399-3054.2006.00674.x.
Zhang, L., Dawes, W., Walker, G., 2001. Response of mean annual evapotranspiration to vegetation changes at catchment scale. Water Resour. Res. 37, 701–708. https://doi.org/10.1029/2000WR900325.
Zhang, L., Hickel, K., Dawes, W.R., Chiew, F.H.S.S., Western, A.W., Briggs, P.R., 2004. A rational function approach for estimating mean annual evapotranspiration. Water Resour. Res. 40, 1–14. https://doi.org/10.1029/2003WR002710.
Zhang, Z., Gong, Y., Wang, Z., 2018. Accessible remote sensing data based reference evapotranspiration estimation modelling. Agric. Water Manag. 210, 59–69. https://doi.org/10.1016/j.agwat.2018.07.039.
Zhang, Z.Z., Zhao, P., McCarthy, H.R., Zhao, X.H., Niu, J.F., Zhu, L.W., Ni, G.Y., Ouyang, L., Huang, Y.Q., 2016. Influence of the decoupling degree on the estimation of canopy stomatal conductance for two broadleaf tree species. Agric. For. Meteorol. 221, 230–241. https://doi.org/10.1016/j.agrformet.2016.02.018.
Zhou, L., Zhou, G., Liu, S., Sui, X., 2010. Seasonal contribution and interannual variation of evapotranspiration over a reed marsh (Phragmites australis)in Northeast China from 3-year eddy covariance data. Hydrol. Process. 24, 1039–1047. https://doi.org/10.1002/hyp.7545.

Agricultural and Forest Meteorology xxx (xxxx) xxx

Contents lists available at ScienceDirect

Agricultural and Forest Meteorology

journal homepage: www.elsevier.com/locate/agrformet

Corrigendum

Corrigendum to "Energy availability and leaf area dominate control of ecosystem evapotranspiration in the southeastern U.S" [Agriculture and Forest Meteorology Volume 349 (2024)/109960]

Maricar Aguilos [a,*], Ge Sun [b], Ning Liu [c], Yulong Zhang [b], Gregory Starr [d], Andrew Christopher Oishi [e], Thomas L O'Halloran [f,j], Jeremy Forsythe [f,j], Jingfeng Wang [g], Modi Zhu [g], Devendra Amatya [h], Benju Baniya [i], Steve McNulty [b], Asko Noormets [i], John King [a]

[a] Department of Forestry and Environmental Resources, North Carolina State University, Raleigh, NC 27695, USA
[b] Eastern Forest Environmental Threat Assessment Center, Southern Research Station, USDA Forest Service, Research Triangle Park, NC, 27709, USA
[c] CSIRO Environment, Canberra, ACT, Australia 2601
[d] Department of Biological Sciences, University of Alabama, Tuscaloosa, AL, 35487, USA
[e] Coweeta Hydrologic Laboratory, Southern Research Station, USDA Forest Service, Otto, NC, 28763 USA
[f] Baruch Institute of Coastal Ecology & Forest Science, Clemson University, Clemson, SC, 29440, USA
[g] School of Civil and Environmental Engineering, Georgia Institute of Technology, Atlanta, GA, 30332, USA
[h] Center for Forest Watershed Research, Southern Research Station, USDA Forest Service, Cordesville, SC, 29434, USA
[i] Department of Ecosystem Science and Management, Texas A&M University, College Station, TX, 77843-2138, USA
[j] Department of Forestry & Environmental Conservation, Clemson University, Clemson, SC, 29634-0317, USA

The authors regret the mistake in Fig. 5a in this article. The authors would like to apologize for any inconvenience caused.

The correct figure is given below.

DOI of original article: https://doi.org/10.1016/j.agrformet.2024.109960.
* Corresponding author at: Maricar Aguilos 2820 Faucette Drive, 1025 Biltmore Hall, Raleigh, NC 27695, USA.
E-mail address: mmaguilo@ncsu.edu (M. Aguilos).

https://doi.org/10.1016/j.agrformet.2024.109986

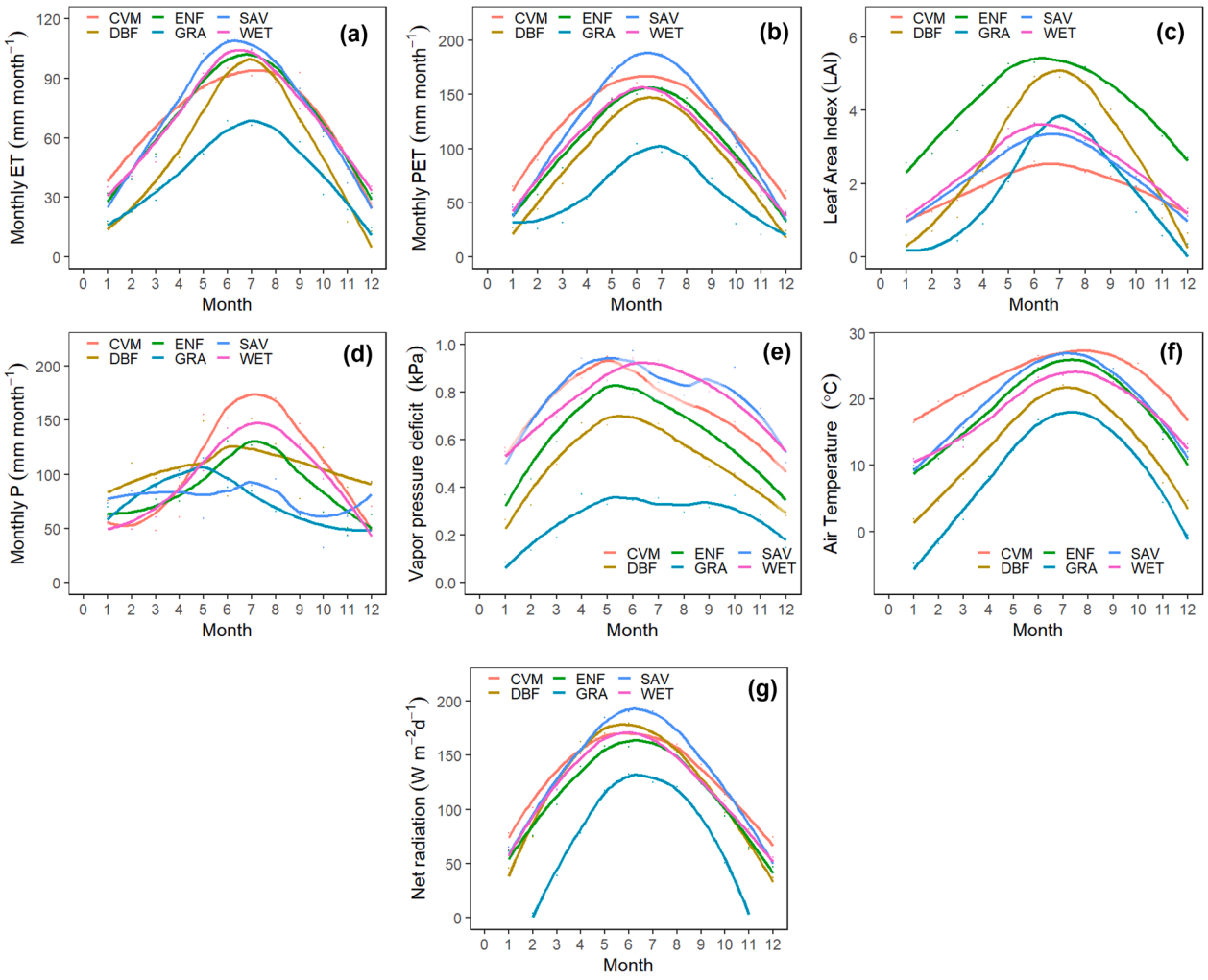

Fig. 5. Variation in biological and climatic input variables, (a) ET (Evapotranspiration), (b) Monthly PET (potential evapotranspiration), (c) LAI (leaf area index), (d) Monthly P (precipitation), (e) VPD (vapour pressure deficit, (f) Tair (air temperature), and (g) Rn (net radiation).